

JAERI-M
90-220

NEANDC (J) -158 / U
INDC (JPN) -146 / L

**MEASUREMENT OF DOUBLE DIFFERENTIAL
NEUTRON EMISSION CROSS SECTIONS AT
14.1 MEV FOR TI, MO AND SN**

December 1990

Akito TAKAHASHI*, Hisashi SUGIMOTO*, Masami GOTOH*,
Ken YAMANAKA*, Haruhito KANAZAWA* and Fujio MAEKAWA

日本原子力研究所
Japan Atomic Energy Research Institute

JAERI-M レポートは、日本原子力研究所が不定期に公刊している研究報告書です。

入手の問合わせは、日本原子力研究所技術情報部情報資料課（〒319-11茨城県那珂郡東海村）
あて、お申しこしください。なお、このほかに財団法人原子力弘済会資料センター（〒319-11茨城
県那珂郡東海村日本原子力研究所内）で複写による実費頒布をおこなっております。

JAERI-M reports are issued irregularly.

Inquiries about availability of the reports should be addressed to Information Division, Department
of Technical Information, Japan Atomic Energy Research Institute, Tokai-mura, Naka-gun,
Ibaraki-ken 319-11, Japan.

© Japan Atomic Energy Research Institute, 1990

編集兼発行 日本原子力研究所
印 刷 日立高速印刷株式会社

Measurement of Double Differential Neutron Emission Cross
Sections at 14.1 MeV for Ti, Mo and Sn

Akito TAKAHASHI*, Hisashi SUGIMOTO*, Masami GOTOH*, Ken YAMANAKA*
Haruhito KANAZAWA* and Fujio MAEKAWA[†]

Department of Physics
Tokai Research Establishment
Japan Atomic Energy Research Institute
Tokai-mura, Naka-gun, Ibaraki-ken

(Received November 16, 1990)

To provide accurate experimental data of double differential neutron emission cross sections at 14.1 MeV which are required for the fusion reactor technology, measurements using the neutron TOF spectrometer at OKTAVIAN have been carried out in these three years under the Research-in-Trust of JAERI. This report describes the results in the third year, for Ti, Mo and Sn.

Data were obtained at 15-16 angle-points in the LAB system for each element and angle-integrated neutron emission spectra were deduced. Angle-differential cross sections were also deduced for elastic and resolved discrete inelastic scatterings. Graphs are given for double differential neutron emission cross sections. Graphs and tables are given for angle-integrated neutron emission spectra and angle-differential cross sections.

Results for Ti and Mo are compared with the JENDL-3 data, and disagreements in the 7-13 MeV region are pointed out. Results for Sn are compared with the ENDL-75 data.

This report is written by summarizing the study implemented under the Research-in-Trust in 1989 fiscal year from the Japan Atomic Energy Research Institute.

* Department of Reactor Engineering

* Osaka University

Keywords : Double Differential Neutron Emission Cross Section, 14.1 MeV,
TOF Measurement, Ti, Mo, Sn, JENDL-3

Ti, Mo, Snの 14.1 MeVにおける
中性子放出二重微分断面積の測定

日本原子力研究所東海研究所物理部
高橋 亮人*・杉本 久司*・後藤 昌美*
山中 健*・金沢 治仁*・前川 藤夫†

(1990年11月16日受理)

核融合炉研究開発に必要な中性子生成の二重微分断面積の 14.1 MeVにおける精度良いデータをうるために、オクタビアンの T O F スペクトロメータを用いて、ここ 3 年間測定を行なってきた。この報告は、最終年度に行なった Ti, Mo, Sn の結果について述べる。 D D X データは、実験室系の 15 – 16 角度点について測定し、角度積分して中性子放出スペクトルが求められた。また、弹性散乱と分離非弹性散乱について角度微分断面積もえられた。

Ti と Mo の結果は、JENDL-3 のデータと比較され、7 – 13 MeV の領域で不一致があることがわかった。Sn の結果は、ENDL-75 のデータと比較された。

本報告書は、日本原子力研究所から平成元年度委託研究で行なわれた成果をまとめたものである。

東海研究所：〒319-11 茨城県那珂郡東海村白方字白根 2-4

+ 原子炉工学部

* 大阪大学

Contents

1.	Introduction	1
2.	Experimental	1
3.	Results	2
3.1	D D X (double differential cross section)	2
3.2	E D X (angle-integrated neutron emission spectrum)	2
3.3	A D X (angle-differential cross section)	2
4.	Discussions	3
	References	4

目 次

1.	序論	1
2.	実験方法	1
3.	結果	2
3.1	D D X (二重微分断面積)	2
3.2	E D X (角度積分された中性子スペクトル)	2
3.3	A D X (角度微分断面積)	2
4.	議論	3
	参考文献	4

1. Introduction

The data base of double differential neutron emission cross sections is useful to assess theoretical nuclear models currently being used in evaluation works of fusion nuclear data, which are required for the nuclear design of Tokamak devices like ITER. Ti and Sn are constituents of super conductors like NbTi and Nb₃Sn. Mo is considered to be used as coating material of diverters. Double differential neutron emission data at 14.1 MeV for these elements are of interest for the estimation of the displacement damages and the kerma factors.

Using the high resolution neutron TOF spectrometer at OKTAVIAN, double differential neutron emission cross sections at 14.1 MeV have been measured for many elements¹⁻³ since 1983. Under the support of JAERI, the autors have carried out experiments for B-10, B-11, Bi-209, Ca, Mn, Co and W^{2,3}. In the present report, results are given for Ti, Mo and Sn.

2. Experimental

The experimental method is described in detail elsewhere⁴. A brief description is given in the following.

The D-T neutron source facility (OKTAVIAN) was operated in pulse mode. The pulse width was 1.8 ns at FWHM and the repetition frequency was 1 MHz. The neutron TOF spectrometer was set along the 85 degree line to the OKTAVIAN beam line and had 8.3 m long flight path. An NE213 detector of 25 cm diameter and 10 cm thickness was set inside a heavy shield at the end of the flight path. The double gain n-gamma discrimination circuit was applied to cover a recoil proton dynamic range of 0.5 MeV to 15 MeV.

The scattering sample (Ti, Mo or Sn) was set along the arc, radially distant by 17 cm from the tritium target. To change the scattering angle, we moved the sample along the arc. Variation of incident neutron energy according to the change of scattering angle was so small that the source energy was regarded as monochromatic (14.1 ± 0.2 MeV). Samples were made of cylindrical metal rods (3 cm in diameter and 7 cm long).

To obtain absolute values of double differential cross sections, a polyethylene sample of 1.5 cm diameter and 5 cm length was used as a reference

1. Introduction

The data base of double differential neutron emission cross sections is useful to assess theoretical nuclear models currently being used in evaluation works of fusion nuclear data, which are required for the nuclear design of Tokamak devices like ITER. Ti and Sn are constituents of super conductors like NbTi and Nb₃Sn. Mo is considered to be used as coating material of diverters. Double differential neutron emission data at 14.1 MeV for these elements are of interest for the estimation of the displacement damages and the kerma factors.

Using the high resolution neutron TOF spectrometer at OKTAVIAN, double differential neutron emission cross sections at 14.1 MeV have been measured for many elements¹⁻³ since 1983. Under the support of JAERI, the autors have carried out experiments for B-10, B-11, Bi-209, Ca, Mn, Co and W^{2,3}. In the present report, results are given for Ti, Mo and Sn.

2. Experimental

The experimental method is described in detail elsewhere⁴. A brief description is given in the following.

The D-T neutron source facility (OKTAVIAN) was operated in pulse mode. The pulse width was 1.8 ns at FWHM and the repetition frequency was 1 MHz. The neutron TOF spectrometer was set along the 85 degree line to the OKTAVIAN beam line and had 8.3 m long flight path. An NE213 detector of 25 cm diameter and 10 cm thickness was set inside a heavy shield at the end of the flight path. The double gain n-gamma discrimination circuit was applied to cover a recoil proton dynamic range of 0.5 MeV to 15 MeV.

The scattering sample (Ti, Mo or Sn) was set along the arc, radially distant by 17 cm from the tritium target. To change the scattering angle, we moved the sample along the arc. Variation of incident neutron energy according to the change of scattering angle was so small that the source energy was regarded as monochromatic (14.1 ± 0.2 MeV). Samples were made of cylindrical metal rods (3 cm in diameter and 7 cm long).

To obtain absolute values of double differential cross sections, a polyethylene sample of 1.5 cm diameter and 5 cm length was used as a reference

scatterer to measure elastically scattered neutron peaks by the H(n,n) reaction at 5 angles from 20 to 50 degree. Absolute efficiency of the NE213 detector was calibrated using these polyethylene data and the differential H(n,n) cross sections of ENDF/B-V. The low energy part (less than 7 MeV) of the efficiency curve was obtained by the TOF experiment using Cf-252 neutron source. Two efficiency curves were normalized in the 5-7 MeV region.

The method of data processing is described in detail elsewhere⁴. To make corrections for multiple scatterings and attenuations, the MUSCC3 code⁵ was used by adopting JENDL-3 data⁶ for Ti and Mo, and ENDL-75 data for Sn⁷.

3. Results

3.1 DDX (double differential cross section)

Obtained double differential neutron emission cross sections for Ti are shown in Fig.T-1 through Fig.T-15, compared with JENDL-3 data. Data for Mo are shown in Fig.M-1 through Fig.M-16, compared with JENDL-3 data. Data for Sn are shown in Fig.S-1 through Fig.S-16, compared with ENDL-75 data.

Numerical data tables of these data will be published in OKTAVIAN Report.

3.2 EDX (angle-integrated neutron emission spectrum)

Measured DDX data at the laboratory angles were converted to those at the center-of-mass system, which were integrated over the CMS angle to deduce EDX data. EDX data in the LAB system were also derived.

Results for Ti are shown in Figs.T-16 and T-17, and in Table 4. Results for Mo are shown in Figs.M-17 and M-18, and in Table 5. Results for Sn are shown in Figs.S-17 and S-18, and in Table 6.

3.3 ADX (angle-differential cross section)

Numerical data are presented for elastic and some resolved angular distributions in Table 1,2 and 3. Resolved data for Ti are for elastic scattering (Fig.T-18), discrete inelastic scattering within a level bin of 0.16-1.794 MeV (Fig.T-19, upper), discrete inelastic scattering of 2.01-2.793 MeV level (Fig.T-19, lower) and discrete inelastic scattering of 3.508-4.16 MeV level

scatterer to measure elastically scattered neutron peaks by the H(n,n) reaction at 5 angles from 20 to 50 degree. Absolute efficiency of the NE213 detector was calibrated using these polyethylene data and the differential H(n,n) cross sections of ENDF/B-V. The low energy part (less than 7 MeV) of the efficiency curve was obtained by the TOF experiment using Cf-252 neutron source. Two efficiency curves were normalized in the 5-7 MeV region.

The method of data processing is described in detail elsewhere⁴. To make corrections for multiple scatterings and attenuations, the MUSCC3 code⁵ was used by adopting JENDL-3 data⁶ for Ti and Mo, and ENDL-75 data for Sn⁷.

3. Results

3.1 DDX (double differential cross section)

Obtained double differential neutron emission cross sections for Ti are shown in Fig.T-1 through Fig.T-15, compared with JENDL-3 data. Data for Mo are shown in Fig.M-1 through Fig.M-16, compared with JENDL-3 data. Data for Sn are shown in Fig.S-1 through Fig.S-16, compared with ENDL-75 data.

Numerical data tables of these data will be published in OKTAVIAN Report.

3.2 EDX (angle-integrated neutron emission spectrum)

Measured DDX data at the laboratory angles were converted to those at the center-of-mass system, which were integrated over the CMS angle to deduce EDX data. EDX data in the LAB system were also derived.

Results for Ti are shown in Figs.T-16 and T-17, and in Table 4. Results for Mo are shown in Figs.M-17 and M-18, and in Table 5. Results for Sn are shown in Figs.S-17 and S-18, and in Table 6.

3.3 ADX (angle-differential cross section)

Numerical data are presented for elastic and some resolved angular distributions in Table 1,2 and 3. Resolved data for Ti are for elastic scattering (Fig.T-18), discrete inelastic scattering within a level bin of 0.16-1.794 MeV (Fig.T-19, upper), discrete inelastic scattering of 2.01-2.793 MeV level (Fig.T-19, lower) and discrete inelastic scattering of 3.508-4.16 MeV level

(Fig.T-20).

ADX data for Mo are obtained for elastic scattering (Fig.M-19), discrete inelastic scattering of 1.4-3.4 MeV level (Fig.M-20, upper) and ($n,2n$) reaction (Fig.M-20, lower).

ADX data for Sn are obtained for elastic scattering (Fig.S-19) and discrete inelastic scattering of 1.9-3.1 MeV level (Fig.S-20).

4. Discussions

From comparisons of DDX data for Ti between the present measurements and the JENDL-3 data, we can say that disagreements are seen in the 3-15 MeV region. In the 1-6 MeV region of E_x (excitation energy), the experiment shows structures probably due to the direct processes and the JENDL-3 data do not reproduce the DDX spectra. Discussions should be similar to the case of Mo.

Comparing all the data of DDX, EDX and ADX for Mo, between the present measurement and the JENDL-3 data, we can say the following;

- 1) The JENDL-3 evaluation is good in the secondary energy region less than 3 MeV. Almost complete agreements are seen in EDX.
- 2) JENDL-3 overestimates differential elastic scattering cross sections in the scattering angle region larger than 40 degree, while good agreements are obtained in forward angles less than 40 degree.
- 3) Though the evaluation is made for the discrete inelastic scattering cross sections of $E_x = 3\text{-}4$ MeV, JENDL-3 gives several orders of magnitude smaller values.
- 4) Neutron emission cross sections of JENDL-3 in the 4-13 MeV region are very underestimated. Choice of calculational parameters for the pre-equilibrium process should be reconsidered, and the use of DWUCK-4 code⁸ for many discrete levels of direct processes is needed. The combinational use of EGNASH⁹, DWUCK-4 code and the Kalbach-Mann systematics¹⁰ is desired to reproduce the measured DDX spectra.
- 5) Measured angle-differential cross sections of ($n,2n$) reaction show slight forward enhancement. Probably due to this fact, the JENDL-3 data slightly overestimate the measured data in the backward angles.

(Fig.T-20).

ADX data for Mo are obtained for elastic scattering (Fig.M-19), discrete inelastic scattering of 1.4-3.4 MeV level (Fig.M-20, upper) and ($n,2n$) reaction (Fig.M-20, lower).

ADX data for Sn are obtained for elastic scattering (Fig.S-19) and discrete inelastic scattering of 1.9-3.1 MeV level (Fig.S-20).

4. Discussions

From comparisons of DDX data for Ti between the present measurements and the JENDL-3 data, we can say that disagreements are seen in the 3-15 MeV region. In the 1-6 MeV region of E_x (excitation energy), the experiment shows structures probably due to the direct processes and the JENDL-3 data do not reproduce the DDX spectra. Discussions should be similar to the case of Mo.

Comparing all the data of DDX, EDX and ADX for Mo, between the present measurement and the JENDL-3 data, we can say the following;

- 1) The JENDL-3 evaluation is good in the secondary energy region less than 3 MeV. Almost complete agreements are seen in EDX.
- 2) JENDL-3 overestimates differential elastic scattering cross sections in the scattering angle region larger than 40 degree, while good agreements are obtained in forward angles less than 40 degree.
- 3) Though the evaluation is made for the discrete inelastic scattering cross sections of $E_x = 3-4$ MeV, JENDL-3 gives several orders of magnitude smaller values.
- 4) Neutron emission cross sections of JENDL-3 in the 4-13 MeV region are very underestimated. Choice of calculational parameters for the pre-equilibrium process should be reconsidered, and the use of DWUCK-4 code⁸ for many discrete levels of direct processes is needed. The combinational use of EGNASH⁹, DWUCK-4 code and the Kalbach-Mann systematics¹⁰ is desired to reproduce the measured DDX spectra.
- 5) Measured angle-differential cross sections of ($n,2n$) reaction show slight forward enhancement. Probably due to this fact, the JENDL-3 data slightly overestimate the measured data in the backward angles.

No evaluations are given for Sn, in JENDL-3. The presently measured data are compared with the ENDL-75 data, which show overall fairly good agreement except the energy region where the measured data show "structures". In future evaluation works for JENDL-upgrade, the combinational use of DWUCK4, EGNASH and the Kalbach-Mann systematics is recommended.

R e f e r e n c e s

- 1) Takahashi, A., et al.: JAERI-M 88-102 (1988)
- 2) Takahashi, A., et al.: JAERI-M 89-214 (1989)
- 3) Takahashi, A., et al.: J. Nucl. Sci. Technol., 26, 15 (1989)
- 4) Takahashi, A., et al.: J. Nucl. Sci. Technol., 25, 215 (1988)
- 5) Ichimura, E., Takahashi, A.: OKTAVIAN Rep. A-87-02, Osaka Univ. (1987)
- 6) Shibata, K., et. al. : JAERI-1319 (1990)
- 7) Howerton, R. J. : Private communication
- 8) Kunz, P. O. :"Distorted Wave Code DUWACK-4", Univ. Colorado (1974)
- 9) Yamamuro, N.: Proc. Nucl. Data Sci. Tech., 1988 Mito, pp.489, Saikou Publ. (1988)
- 10) Kalbach, C., Mann, F.M.G.: Phys. Rev., C23, 112 (1981)

No evaluations are given for Sn, in JENDL-3. The presently measured data are compared with the ENDL-75 data, which show overall fairly good agreement except the energy region where the measured data show "structures". In future evaluation works for JENDL-upgrade, the combinational use of DWUCK4, EGNASH and the Kalbach-Mann systematics is recommended.

R e f e r e n c e s

- 1) Takahashi, A., et al.: JAERI-M 88-102 (1988)
- 2) Takahashi, A., et al.: JAERI-M 89-214 (1989)
- 3) Takahashi, A., et al.: J. Nucl. Sci. Technol., 26, 15 (1989)
- 4) Takahashi, A., et al.: J. Nucl. Sci. Technol., 25, 215 (1988)
- 5) Ichimura, E., Takahashi, A.: OKTAVIAN Rep. A-87-02, Osaka Univ. (1987)
- 6) Shibata, K., et. al. : JAERI-1319 (1990)
- 7) Howerton, R. J. : Private communication
- 8) Kunz, P. O. :"Distorted Wave Code DUWACK-4", Univ. Colorado (1974)
- 9) Yamamuro, N.: Proc. Nucl. Data Sci. Tech., 1988 Mito, pp.489, Saikou Publ. (1988)
- 10) Kalbach, C., Mann, F.M.G.: Phys. Rev., C23, 112 (1981)

Table 1 Partial differential cross sections for titanium at 14.1 MeV

$\theta_{\text{L}^{\text{A}}\text{B}}$ (deg)	elastic		$Q = -0.16 \sim -1.8 \text{ MeV}$		$Q = -2.0 \sim -2.1 \text{ MeV}$		$Q = -3.5 \sim -4.2 \text{ MeV}$	
	$d\sigma/d\Omega$ (b/sr)	error	$d\sigma/d\Omega$ (b/sr)	error	$d\sigma/d\Omega$ (b/sr)	error	$d\sigma/d\Omega$ (b/sr)	error
15	3.62E-3	1.1E-4	—	—	—	—	7.99E-4	1.4E-4
20	2.13E-3	6.4E-5	—	—	—	—	5.05E-4	9.1E-5
30	9.57E-4	2.9E-5	—	—	—	—	3.04E-4	5.5E-5
40	4.37E-4	1.3E-5	1.89E-4	4.7E-5	1.49E-4	4.5E-5	2.00E-4	3.6E-5
50	3.83E-4	1.5E-5	1.83E-4	4.6E-5	1.39E-4	4.2E-5	2.00E-4	3.6E-5
70	3.28E-4	1.3E-5	1.63E-4	4.1E-5	1.21E-4	4.2E-5	1.83E-4	3.3E-5
80	2.11E-4	6.3E-6	1.10E-4	2.8E-5	8.00E-5	2.4E-5	1.20E-4	2.4E-5
90	3.60E-4	1.1E-5	1.79E-4	4.5E-5	1.38E-4	4.8E-5	1.93E-4	3.5E-5
100	1.44E-4	4.3E-6	8.29E-5	2.1E-4	6.10E-5	1.8E-5	9.01E-5	1.8E-5
110	2.12E-4	6.4E-6	1.26E-4	3.3E-5	1.15E-4	4.0E-5	1.65E-4	3.0E-5
120	2.18E-4	6.5E-6	1.54E-4	3.9E-5	1.26E-4	4.4E-5	1.83E-4	3.3E-5
130	1.85E-4	5.6E-6	1.19E-4	3.0E-5	1.07E-4	3.7E-5	1.62E-4	2.9E-5
140	1.93E-4	5.8E-6	1.23E-4	3.2E-5	1.15E-4	4.0E-5	1.74E-4	3.1E-5
150	2.39E-4	7.2E-6	1.56E-4	4.4E-5	1.44E-4	5.0E-5	2.34E-4	5.6E-5
160	4.12E-4	1.2E-5	2.83E-4	8.0E-5	3.00E-4	1.2E-4	4.72E-4	1.1E-4
σ_{tot} (b)	9.01E-1	4.5E-2	7.09E-2	2.1E-2	2.55E-2	9.7E-3	7.22E-2	1.8E-2

Table 2 Partial differential cross sections for molybdenum at 14.1 MeV

θ_{LAB} (deg)	elastic		$Q = -1.4 \sim -3.4$ MeV		(n, 2n)	
	$d\sigma/d\Omega$ (b/sr)	error	$d\sigma/d\Omega$ (b/sr)	error	$d\sigma/d\Omega$ (b/sr)	error
15	3.95E+0	1.2E-1	—	—	1.95E-1	1.2E-2
20	1.74E+0	5.2E-2	—	—	1.78E-1	1.1E-2
30	4.59E-1	1.4E-2	—	—	1.85E-1	1.1E-2
40	2.20E-2	6.6E-3	9.84E-3	3.0E-3	1.82E-1	1.1E-2
50	3.15E-2	9.5E-4	9.61E-3	2.4E-3	1.68E-1	1.0E-2
60	3.03E-2	9.1E-4	9.07E-3	1.8E-3	1.79E-1	1.1E-2
70	3.04E-2	1.2E-3	7.64E-3	1.5E-3	1.55E-1	1.2E-2
80	1.26E-2	3.8E-4	6.00E-3	1.2E-3	1.58E-1	9.5E-3
90	7.98E-3	2.4E-4	5.31E-3	1.1E-3	1.49E-1	9.0E-3
100	1.33E-2	4.0E-4	4.95E-3	9.9E-4	1.52E-1	9.1E-3
110	1.49E-2	4.5E-4	3.88E-3	7.8E-4	1.39E-1	8.4E-3
120	6.92E-3	2.1E-4	3.56E-3	8.9E-4	1.33E-1	8.0E-3
130	7.90E-3	2.4E-4	4.15E-3	8.3E-4	1.38E-1	8.3E-3
140	7.90E-3	2.4E-4	3.60E-3	1.1E-3	1.63E-1	9.8E-3
150	7.64E-3	3.1E-4	4.54E-3	1.4E-3	1.47E-1	1.0E-2
160	1.47E-2	5.9E-4	4.45E-3	1.3E-3	1.47E-1	1.0E-2
σ_{total} (b)	2.51E+0	2.5E-1	8.00E-2	1.6E-2	1.95E+0	1.4E-1

Table 3 Partial differential cross sections for tin at En=14.1 MeV

θ_{LAB} (deg)	elastic		$Q = -1.4 \sim -3.4 \text{ MeV}$	
	$d\sigma/d\Omega$ (b/sr)	error	$d\sigma/d\Omega$ (b/sr)	error
15	3.37E+0	1.0E-1	—	—
20	1.68E+0	5.0E-2	—	—
30	3.44E-1	1.0E-2	1.22E-2	2.4E-3
40	6.20E-2	1.9E-3	9.63E-3	1.9E-3
50	8.01E-2	2.4E-3	8.56E-3	1.7E-3
60	3.63E-2	1.1E-3	5.71E-3	1.1E-3
70	1.93E-2	5.8E-4	5.98E-3	1.2E-3
80	1.37E-2	4.1E-4	4.88E-3	9.8E-4
90	1.36E-2	6.8E-4	4.55E-3	9.1E-4
100	1.71E-2	5.1E-4	3.54E-3	7.1E-4
110	1.05E-2	3.2E-4	2.94E-3	5.9E-4
120	5.19E-3	1.6E-4	2.55E-3	5.1E-4
130	5.43E-3	1.6E-4	3.00E-3	6.0E-4
140	9.84E-3	3.0E-4	2.19E-3	5.5E-4
150	7.96E-3	2.4E-4	2.21E-3	6.6E-4
160	8.11E-3	2.4E-4	4.04E-3	1.2E-3
$\sigma_{\text{total}}(\text{b})$	—	—	6.73E-2	1.7E-2

Table 4 Angle-integrated neutron emission spectra for Ti

SUBENTRY	00025003	900201	00025003			
BIB	2	8	00025003			
COMMENT	TWO DATA SETS ARE GIVEN.					
	DATA OBTAINED FROM RAW DDX DATA , IN LEFT HAND SIDE.					
	DATA OBTAINED FROM CORRECTED DDX DATA WITH MUSCC3 CODE					
REACTION	(22-TI-0(N,SCT),,,DE) SECONDARY NEUTRON SPECTRUM					
	IN THE CENTER-OF-MASS SYSTEM					
ENDBIB	8		00025003			
COMMON	1	5	00025003			
EN			00025003			
MEV			00025003			
14.10000			00025003			
ENDCOMMON	5		00025003			
DATA	6	69	00025003			
E-MAX	E-MIN	DATA	DATA-ERR	DATA	DATA-ERR	00025003
MEV	MEV	B/MEV	B/MEV	B/MEV	B/MEV	00025003
14.60000	14.40000	5.95E-02	4.59E-03	6.39E-02	4.77E-03	00025003
14.40000	14.20000	1.49E-01	3.51E-03	1.68E-01	3.73E-03	00025003
14.20000	14.00000	4.06E-01	2.30E-03	4.63E-01	2.39E-03	00025003
14.00000	13.80000	8.06E-01	2.69E-03	9.21E-01	2.88E-03	00025003
13.80000	13.60000	1.03E+00	2.81E-03	1.17E+00	3.06E-03	00025003
13.60000	13.40000	9.03E-01	2.63E-03	1.03E+00	2.89E-03	00025003
13.40000	13.20000	6.08E-01	2.24E-03	6.88E-01	2.46E-03	00025003
13.20000	13.00000	3.61E-01	1.82E-03	4.07E-01	1.98E-03	00025003
13.00000	12.80000	2.13E-01	1.51E-03	2.40E-01	1.66E-03	00025003
12.80000	12.60000	1.52E-01	1.36E-03	1.71E-01	1.50E-03	00025003
12.60000	12.40000	1.17E-01	1.26E-03	1.32E-01	1.40E-03	00025003
12.40000	12.20000	8.38E-02	1.14E-03	9.39E-02	1.26E-03	00025003
12.20000	12.00000	5.90E-02	1.05E-03	6.57E-02	1.15E-03	00025003
12.00000	11.80000	4.27E-02	9.84E-04	4.76E-02	1.07E-03	00025003
11.80000	11.60000	3.47E-02	9.31E-04	3.86E-02	1.00E-03	00025003
11.60000	11.40000	3.37E-02	9.00E-04	3.75E-02	9.78E-04	00025003
11.40000	11.20000	3.41E-02	8.83E-04	3.79E-02	9.67E-04	00025003
11.20000	11.00000	3.18E-02	8.52E-04	3.53E-02	9.37E-04	00025003
11.00000	10.80000	2.89E-02	8.23E-04	3.22E-02	9.06E-04	00025003
10.80000	10.60000	3.00E-02	8.25E-04	3.35E-02	9.12E-04	00025003
10.60000	10.40000	3.62E-02	8.49E-04	4.03E-02	9.41E-04	00025003
10.40000	10.20000	4.23E-02	8.76E-04	4.72E-02	9.74E-04	00025003
10.20000	10.00000	4.28E-02	8.74E-04	4.76E-02	9.71E-04	00025003
10.00000	9.80000	3.84E-02	8.51E-04	4.27E-02	9.45E-04	00025003
9.80000	9.60000	3.46E-02	8.44E-04	3.85E-02	9.36E-04	00025003
9.60000	9.40000	3.23E-02	8.34E-04	3.59E-02	9.26E-04	00025003
9.40000	9.20000	3.15E-02	8.40E-04	3.46E-02	9.24E-04	00025003
9.20000	9.00000	3.01E-02	8.37E-04	2.99E-02	8.45E-04	00025003
9.00000	8.80000	3.05E-02	8.45E-04	2.95E-02	8.41E-04	00025003
8.80000	8.60000	2.97E-02	8.51E-04	2.86E-02	8.49E-04	00025003
8.60000	8.40000	2.83E-02	8.45E-04	2.79E-02	8.55E-04	00025003
8.40000	8.20000	2.98E-02	8.60E-04	2.98E-02	8.70E-04	00025003
8.20000	8.00000	3.11E-02	8.64E-04	3.14E-02	8.80E-04	00025003
8.00000	7.80000	3.49E-02	8.74E-04	3.53E-02	8.91E-04	00025003
7.80000	7.60000	3.61E-02	8.86E-04	3.69E-02	9.10E-04	00025003
7.60000	7.40000	3.87E-02	8.96E-04	3.98E-02	9.23E-04	00025003
7.40000	7.20000	4.15E-02	9.03E-04	4.28E-02	9.31E-04	00025003
7.20000	7.00000	4.41E-02	9.05E-04	4.58E-02	9.36E-04	00025003
7.00000	6.80000	4.45E-02	9.09E-04	4.67E-02	9.43E-04	00025003
6.80000	6.60000	4.58E-02	9.09E-04	4.76E-02	9.42E-04	00025003
6.60000	6.40000	4.75E-02	9.02E-04	4.95E-02	9.38E-04	00025003
6.40000	6.20000	5.00E-02	9.05E-04	5.19E-02	9.43E-04	00025003
6.20000	6.00000	5.31E-02	9.18E-04	5.53E-02	9.59E-04	00025003
6.00000	5.80000	5.62E-02	9.27E-04	5.88E-02	9.70E-04	00025003
5.80000	5.60000	6.06E-02	9.38E-04	6.36E-02	9.85E-04	00025003
5.60000	5.40000	6.42E-02	9.43E-04	6.75E-02	9.92E-04	00025003
5.40000	5.20000	6.82E-02	9.63E-04	7.17E-02	1.01E-03	00025003
5.20000	5.00000	7.48E-02	9.84E-04	7.89E-02	1.04E-03	00025003
5.00000	4.80000	8.01E-02	9.98E-04	8.44E-02	1.05E-03	00025003
4.80000	4.60000	8.80E-02	1.01E-03	9.25E-02	1.06E-03	00025003
4.60000	4.40000	9.44E-02	1.03E-03	9.90E-02	1.08E-03	00025003
4.40000	4.20000	1.01E-01	1.05E-03	1.06E-01	1.10E-03	00025003
4.20000	4.00000	1.11E-01	1.08E-03	1.16E-01	1.13E-03	00025003
4.00000	3.80000	1.19E-01	1.10E-03	1.24E-01	1.15E-03	00025003
3.80000	3.60000	1.28E-01	1.13E-03	1.34E-01	1.18E-03	00025003
3.60000	3.40000	1.38E-01	1.16E-03	1.44E-01	1.21E-03	00025003
3.40000	3.20000	1.49E-01	1.19E-03	1.55E-01	1.23E-03	00025003
3.20000	3.00000	1.66E-01	1.24E-03	1.71E-01	1.28E-03	00025003
3.00000	2.80000	1.80E-01	1.31E-03	1.85E-01	1.35E-03	00025003
2.80000	2.60000	1.96E-01	1.37E-03	2.01E-01	1.41E-03	00025003
2.60000	2.40000	2.24E-01	1.46E-03	2.28E-01	1.49E-03	00025003
2.40000	2.20000	2.56E-01	1.56E-03	2.58E-01	1.57E-03	00025003
2.20000	2.00000	2.74E-01	1.64E-03	2.73E-01	1.64E-03	00025003
2.00000	1.80000	3.06E-01	1.73E-03	3.03E-01	1.70E-03	00025003
1.80000	1.60000	3.41E-01	1.88E-03	3.33E-01	1.82E-03	00025003
1.60000	1.40000	3.89E-01	2.14E-03	3.77E-01	2.07E-03	00025003
1.40000	1.20000	4.46E-01	2.75E-03	4.27E-01	2.62E-03	00025003
1.20000	1.00000	4.59E-01	4.20E-03	4.32E-01	3.96E-03	00025003
1.00000	0.80000	4.09E-01	6.52E-03	3.78E-01	6.04E-03	00025003
ENDDATA	73		00025003			
ENDSUBENTRY	88		0002500399999			
ENDENTRY	3		0002599999999			

Table 5 Angle-integrated neutron emission spectra for Mo

SUBENTRY	00024003	900201	00024003	1				
BIB	2	8	00024003	2				
COMMENT	TWO DATA SETS ARE GIVEN.			3				
	DATA OBTAINED FROM RAW DDX DATA , IN LEFT HAND SIDE.			4				
	DATA OBTAINED FROM CORRECTED DDX DATA WITH MUSCC3 CODE			5				
	IN RIGHT HAND SIDE.			6				
REACTION	(42-MO-0(N,SCT),,DE) SECONDARY NEUTRON SPECTRUM			7				
	IN THE CENTER-OF-MASS SYSTEM			8				
ENDBIB	8		00024003	9				
COMMON	1	5	00024003	10				
EN			00024003	11				
MEV			00024003	12				
14.10000			00024003	13				
ENDCOMMON	5		00024003	14				
DATA	6	68	00024003	15				
E-MAX	E-MIN	DATA	DATA-ERR	DATA	DATA-ERR	DATA-ERR	00024003	16
MEV	MEV	B/MEV	B/MEV	B/MEV	B/MEV	B/MEV	00024003	17
14.80000	14.60000	5.62E-02	3.09E-03	5.60E-02	3.52E-03	0.00024003	18	
14.60000	14.40000	3.17E-01	4.19E-03	3.56E-01	4.85E-03	0.00024003	19	
14.40000	14.20000	7.94E-01	2.60E-03	1.03E+00	3.05E-03	0.00024003	20	
14.20000	14.00000	1.85E+00	3.30E-03	2.40E+00	3.97E-03	0.00024003	21	
14.00000	13.80000	2.52E+00	3.56E-03	3.26E+00	4.35E-03	0.00024003	22	
13.80000	13.60000	2.11E+00	3.15E-03	2.70E+00	3.81E-03	0.00024003	23	
13.60000	13.40000	1.18E+00	2.37E-03	1.50E+00	2.79E-03	0.00024003	24	
13.40000	13.20000	5.23E-01	1.76E-03	6.47E+00	1.98E-03	0.00024003	25	
13.20000	13.00000	2.51E-01	1.42E-03	3.04E-01	1.55E-03	0.00024003	26	
13.00000	12.80000	1.56E-01	1.24E-03	1.88E-01	1.38E-03	0.00024003	27	
12.80000	12.60000	1.06E-01	1.12E-03	1.30E-01	1.27E-03	0.00024003	28	
12.60000	12.40000	7.68E-02	1.04E-03	9.56E-02	1.19E-03	0.00024003	29	
12.40000	12.20000	6.34E-02	1.00E-03	7.84E-02	1.16E-03	0.00024003	30	
12.20000	12.00000	5.89E-02	9.83E-04	7.14E-02	1.13E-03	0.00024003	31	
12.00000	11.80000	6.32E-02	9.76E-04	7.45E-02	1.11E-03	0.00024003	32	
11.80000	11.60000	6.40E-02	9.64E-04	7.46E-02	1.11E-03	0.00024003	33	
11.60000	11.40000	5.96E-02	9.37E-04	6.97E-02	1.08E-03	0.00024003	34	
11.40000	11.20000	5.41E-02	8.99E-04	6.35E-02	1.05E-03	0.00024003	35	
11.20000	11.00000	5.03E-02	8.71E-04	5.99E-02	1.03E-03	0.00024003	36	
11.00000	10.80000	4.41E-02	8.39E-04	5.26E-02	9.97E-04	0.00024003	37	
10.80000	10.60000	3.70E-02	8.15E-04	4.46E-02	9.72E-04	0.00024003	38	
10.60000	10.40000	3.02E-02	7.94E-04	3.65E-02	9.50E-04	0.00024003	39	
10.40000	10.20000	2.87E-02	7.86E-04	3.47E-02	9.41E-04	0.00024003	40	
10.20000	10.00000	2.94E-02	7.82E-04	3.59E-02	9.42E-04	0.00024003	41	
10.00000	9.80000	2.91E-02	7.94E-04	3.55E-02	9.55E-04	0.00024003	42	
9.80000	9.60000	2.78E-02	7.84E-04	3.36E-02	9.42E-04	0.00024003	43	
9.60000	9.40000	2.81E-02	7.86E-04	3.32E-02	9.25E-04	0.00024003	44	
9.40000	9.20000	2.77E-02	7.91E-04	2.42E-02	7.69E-04	0.00024003	45	
9.20000	9.00000	2.76E-02	7.95E-04	2.23E-02	7.64E-04	0.00024003	46	
9.00000	8.80000	2.85E-02	8.03E-04	2.44E-02	7.78E-04	0.00024003	47	
8.80000	8.60000	2.74E-02	8.12E-04	2.45E-02	7.95E-04	0.00024003	48	
8.60000	8.40000	2.81E-02	8.17E-04	2.53E-02	8.05E-04	0.00024003	49	
8.40000	8.20000	2.81E-02	8.30E-04	2.60E-02	8.30E-04	0.00024003	50	
8.20000	8.00000	3.12E-02	8.46E-04	2.93E-02	8.53E-04	0.00024003	51	
8.00000	7.80000	3.07E-02	8.50E-04	2.96E-02	8.64E-04	0.00024003	52	
7.80000	7.60000	2.98E-02	8.56E-04	2.93E-02	8.73E-04	0.00024003	53	
7.60000	7.40000	3.32E-02	8.65E-04	3.29E-02	8.83E-04	0.00024003	54	
7.40000	7.20000	3.53E-02	8.65E-04	3.47E-02	8.87E-04	0.00024003	55	
7.20000	7.00000	3.65E-02	8.66E-04	3.70E-02	8.87E-04	0.00024003	56	
7.00000	6.80000	3.70E-02	8.65E-04	3.77E-02	8.90E-04	0.00024003	57	
6.80000	6.60000	3.93E-02	8.68E-04	4.02E-02	9.01E-04	0.00024003	58	
6.60000	6.40000	4.25E-02	8.64E-04	4.31E-02	9.03E-04	0.00024003	59	
6.40000	6.20000	4.47E-02	8.67E-04	4.59E-02	9.07E-04	0.00024003	60	
6.20000	6.00000	4.58E-02	8.72E-04	4.76E-02	9.23E-04	0.00024003	61	
6.00000	5.80000	4.84E-02	8.76E-04	5.11E-02	9.32E-04	0.00024003	62	
5.80000	5.60000	4.94E-02	8.87E-04	5.26E-02	9.52E-04	0.00024003	63	
5.60000	5.40000	5.22E-02	8.94E-04	5.63E-02	9.64E-04	0.00024003	64	
5.40000	5.20000	5.83E-02	9.03E-04	6.33E-02	9.78E-04	0.00024003	65	
5.20000	5.00000	6.28E-02	9.04E-04	6.83E-02	9.85E-04	0.00024003	66	
5.00000	4.80000	6.85E-02	9.19E-04	7.50E-02	1.01E-03	0.00024003	67	
4.80000	4.60000	7.61E-02	9.31E-04	8.39E-02	1.03E-03	0.00024003	68	
4.60000	4.40000	8.33E-02	9.44E-04	9.31E-02	1.05E-03	0.00024003	69	
4.40000	4.20000	9.44E-02	9.63E-04	1.06E-01	1.08E-03	0.00024003	70	
4.20000	4.00000	1.04E-01	9.84E-04	1.18E-01	1.11E-03	0.00024003	71	
4.00000	3.80000	1.16E-01	9.99E-04	1.32E-01	1.14E-03	0.00024003	72	
3.80000	3.60000	1.28E-01	1.03E-03	1.47E-01	1.18E-03	0.00024003	73	
3.60000	3.40000	1.45E-01	1.05E-03	1.67E-01	1.21E-03	0.00024003	74	
3.40000	3.20000	1.67E-01	1.10E-03	1.93E-01	1.27E-03	0.00024003	75	
3.20000	3.00000	1.95E-01	1.15E-03	2.25E-01	1.33E-03	0.00024003	76	
3.00000	2.80000	2.22E-01	1.21E-03	2.57E-01	1.41E-03	0.00024003	77	
2.80000	2.60000	2.60E-01	1.30E-03	2.99E-01	1.51E-03	0.00024003	78	
2.60000	2.40000	3.09E-01	1.45E-03	3.54E-01	1.68E-03	0.00024003	79	
2.40000	2.20000	3.64E-01	1.53E-03	4.18E-01	1.77E-03	0.00024003	80	
2.20000	2.00000	4.21E-01	1.67E-03	4.85E-01	1.93E-03	0.00024003	81	
2.00000	1.80000	4.83E-01	1.88E-03	5.56E-01	2.18E-03	0.00024003	82	
1.80000	1.60000	5.60E-01	2.33E-03	6.43E-01	2.69E-03	0.00024003	83	
1.60000	1.40000	6.99E-01	3.64E-03	8.00E-01	4.20E-03	0.00024003	84	
1.40000	1.20000	7.26E-01	6.86E-03	8.30E-01	7.91E-03	0.00024003	85	
ENDDATA	72				00024003		86	
ENDSUBENTRY	87				00024003999999			
ENDENTRY	3				00024999999999			

Table 6 Angle-integrated neutron emission spectra for Sn

SUBENTRY	00026003	900401	00026003	1			
BIB	2	8	00026003	2			
COMMENT	TWO DATA SETS ARE GIVEN.			3			
	DATA OBTAINED FROM RAW DDX DATA , IN LEFT HAND SIDE.			4			
	DATA OBTAINED FROM CORRECTED DDX DATA WITH MUSCC3 CODE			5			
	IN RIGHT HAND SIDE.			6			
REACTION	(50-SN-0(N,SCT)...,DE) SECONDARY NEUTRON SPECTRUM			7			
	IN THE CENTER-OF-MASS SYSTEM			8			
ENDBIB	8		00026003	9			
COMMON	1	5	00026003	10			
EN			00026003	11			
MEV			00026003	12			
14.10000			00026003	13			
ENDCOMMON	5		00026003	14			
DATA	6	70	00026003	15			
E-MAX	E-MIN	DATA	DATA-ERR	DATA	DATA-ERR	00026003	16
MEV	MEV	B/MEV	B/MEV	B/MEV	B/MEV	00026003	17
14.80000	14.60000	9.97E-02	3.34E-03	1.11E-01	3.58E-03000026003	18	
14.60000	14.40000	3.69E-01	4.14E-03	4.11E-01	4.18E-03000026003	19	
14.40000	14.20000	1.07E+00	4.00E-03	1.19E+00	4.20E-03000026003	20	
14.20000	14.00000	1.92E+00	5.02E-03	2.12E+00	5.29E-03000026003	21	
14.00000	13.80000	2.27E+00	5.00E-03	2.50E+00	5.24E-03000026003	22	
13.80000	13.60000	1.92E+00	4.50E-03	2.12E+00	4.72E-03000026003	23	
13.60000	13.40000	1.25E+00	3.67E-03	1.38E+00	3.82E-03000026003	24	
13.40000	13.20000	6.95E-01	2.91E-03	7.71E-01	3.02E-03000026003	25	
13.20000	13.00000	3.85E-01	2.38E-03	4.10E-01	2.40E-03000026003	26	
13.00000	12.80000	2.35E-01	2.08E-03	2.63E-01	2.19E-03000026003	27	
12.80000	12.60000	1.67E-01	1.91E-03	1.87E-01	2.03E-03000026003	28	
12.60000	12.40000	1.24E-01	1.77E-03	1.38E-01	1.88E-03000026003	29	
12.40000	12.20000	9.41E-02	1.64E-03	1.06E-01	1.76E-03000026003	30	
12.20000	12.00000	7.56E-02	1.56E-03	8.47E-02	1.68E-03000026003	31	
12.00000	11.80000	7.45E-02	1.52E-03	8.29E-02	1.64E-03000026003	32	
11.80000	11.60000	8.74E-02	1.52E-03	9.61E-02	1.64E-03000026003	33	
11.60000	11.40000	8.98E-02	1.51E-03	9.87E-02	1.64E-03000026003	34	
11.40000	11.20000	7.76E-02	1.44E-03	8.51E-02	1.57E-03000026003	35	
11.20000	11.00000	6.08E-02	1.35E-03	6.67E-02	1.47E-03000026003	36	
11.00000	10.80000	4.79E-02	1.29E-03	5.27E-02	1.40E-03000026003	37	
10.80000	10.60000	4.20E-02	1.26E-03	4.59E-02	1.36E-03000026003	38	
10.60000	10.40000	3.74E-02	1.24E-03	4.08E-02	1.35E-03000026003	39	
10.40000	10.20000	3.73E-02	1.24E-03	4.06E-02	1.35E-03000026003	40	
10.20000	10.00000	3.45E-02	1.22E-03	3.75E-02	1.33E-03000026003	41	
10.00000	9.80000	3.36E-02	1.21E-03	3.67E-02	1.32E-03000026003	42	
9.80000	9.60000	3.14E-02	1.20E-03	3.46E-02	1.32E-03000026003	43	
9.60000	9.40000	3.42E-02	1.22E-03	3.69E-02	1.32E-03000026003	44	
9.40000	9.20000	3.48E-02	1.23E-03	3.07E-02	1.20E-03000026003	45	
9.20000	9.00000	3.64E-02	1.23E-03	3.16E-02	1.20E-03000026003	46	
9.00000	8.80000	3.86E-02	1.25E-03	3.35E-02	1.22E-03000026003	47	
8.80000	8.60000	3.69E-02	1.27E-03	3.35E-02	1.24E-03000026003	48	
8.60000	8.40000	3.70E-02	1.29E-03	3.43E-02	1.26E-03000026003	49	
8.40000	8.20000	3.50E-02	1.29E-03	3.29E-02	1.27E-03000026003	50	
8.20000	8.00000	3.63E-02	1.30E-03	3.49E-02	1.29E-03000026003	51	
8.00000	7.80000	3.69E-02	1.30E-03	3.55E-02	1.30E-03000026003	52	
7.80000	7.60000	3.74E-02	1.30E-03	3.62E-02	1.30E-03000026003	53	
7.60000	7.40000	4.18E-02	1.31E-03	4.06E-02	1.32E-03000026003	54	
7.40000	7.20000	4.69E-02	1.32E-03	4.65E-02	1.32E-03000026003	55	
7.20000	7.00000	4.64E-02	1.31E-03	4.55E-02	1.31E-03000026003	56	
7.00000	6.80000	4.98E-02	1.30E-03	4.78E-02	1.29E-03000026003	57	
6.80000	6.60000	5.20E-02	1.30E-03	4.96E-02	1.30E-03000026003	58	
6.60000	6.40000	5.21E-02	1.31E-03	4.99E-02	1.30E-03000026003	59	
6.40000	6.20000	5.39E-02	1.32E-03	5.16E-02	1.31E-03000026003	60	
6.20000	6.00000	5.59E-02	1.32E-03	5.35E-02	1.32E-03000026003	61	
6.00000	5.80000	5.46E-02	1.33E-03	5.34E-02	1.34E-03000026003	62	
5.80000	5.60000	5.66E-02	1.35E-03	5.56E-02	1.36E-03000026003	63	
5.60000	5.40000	5.86E-02	1.36E-03	5.83E-02	1.39E-03000026003	64	
5.40000	5.20000	5.99E-02	1.39E-03	5.99E-02	1.42E-03000026003	65	
5.20000	5.00000	6.95E-02	1.41E-03	6.97E-02	1.44E-03000026003	66	
5.00000	4.80000	7.73E-02	1.44E-03	7.76E-02	1.46E-03000026003	67	
4.80000	4.60000	8.70E-02	1.47E-03	8.74E-02	1.51E-03000026003	68	
4.60000	4.40000	9.72E-02	1.51E-03	9.89E-02	1.57E-03000026003	69	
4.40000	4.20000	1.06E-01	1.54E-03	1.09E-01	1.60E-03000026003	70	
4.20000	4.00000	1.20E-01	1.59E-03	1.23E-01	1.66E-03000026003	71	
4.00000	3.80000	1.34E-01	1.64E-03	1.36E-01	1.70E-03000026003	72	
3.80000	3.60000	1.50E-01	1.70E-03	1.53E-01	1.75E-03000026003	73	
3.60000	3.40000	1.75E-01	1.76E-03	1.78E-01	1.82E-03000026003	74	
3.40000	3.20000	2.04E-01	1.85E-03	2.09E-01	1.92E-03000026003	75	
3.20000	3.00000	2.43E-01	1.96E-03	2.47E-01	2.01E-03000026003	76	
3.00000	2.80000	2.93E-01	2.10E-03	2.89E-01	2.09E-03000026003	77	
2.80000	2.60000	3.51E-01	2.28E-03	3.45E-01	2.27E-03000026003	78	
2.60000	2.40000	4.26E-01	2.52E-03	4.19E-01	2.52E-03000026003	79	
2.40000	2.20000	5.21E-01	2.63E-03	5.19E-01	2.64E-03000026003	80	
2.20000	2.00000	6.26E-01	2.83E-03	6.28E-01	2.87E-03000026003	81	
2.00000	1.80000	7.60E-01	3.12E-03	7.56E-01	3.13E-03000026003	82	
1.80000	1.60000	9.19E-01	3.43E-03	9.08E-01	3.43E-03000026003	83	
1.60000	1.40000	1.09E+00	3.91E-03	1.08E+00	3.89E-03000026003	84	
1.40000	1.20000	1.28E+00	4.59E-03	1.25E+00	4.56E-03000026003	85	
1.20000	1.00000	1.57E+00	7.17E-03	1.51E+00	7.13E-03000026003	86	
1.00000	0.80000	1.68E+00	8.41E-03	1.57E+00	7.94E-03000026003	87	
ENDDATA	74		00026003	88			
ENDSUBENTRY	89		00026003999999				
ENDENTRY	3		00026999999999				

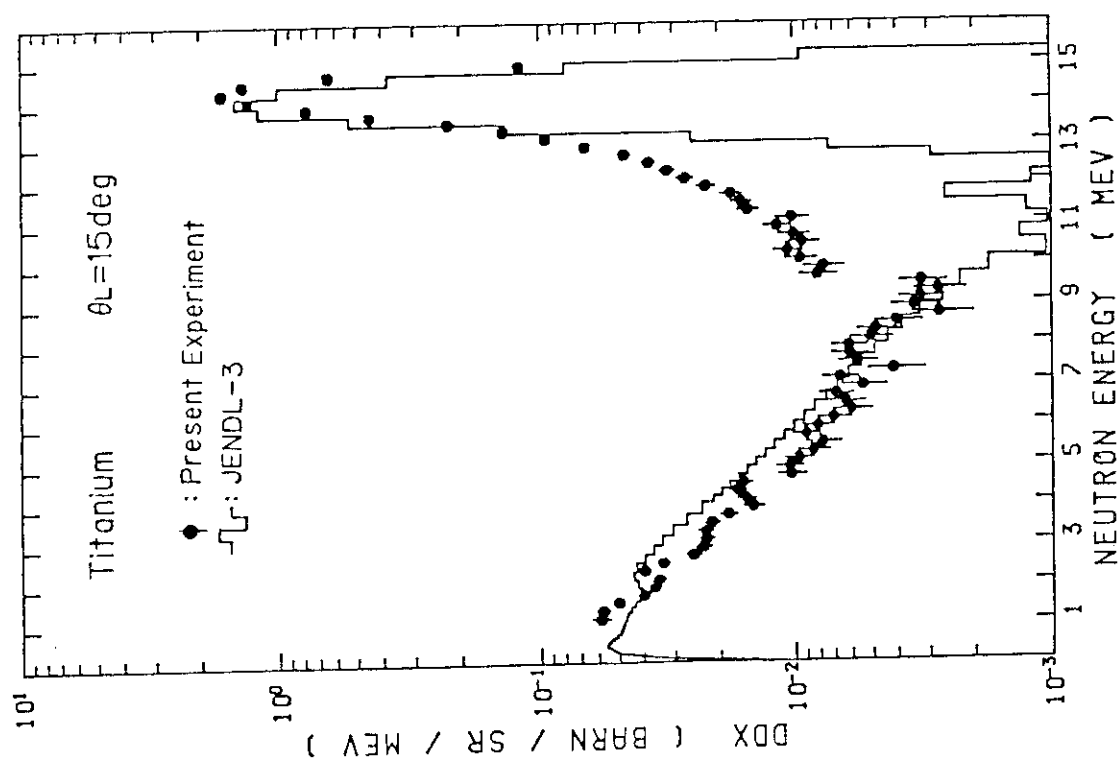


Fig.T-1 Double differential neutron emission cross sections at 15 deg, for Ti

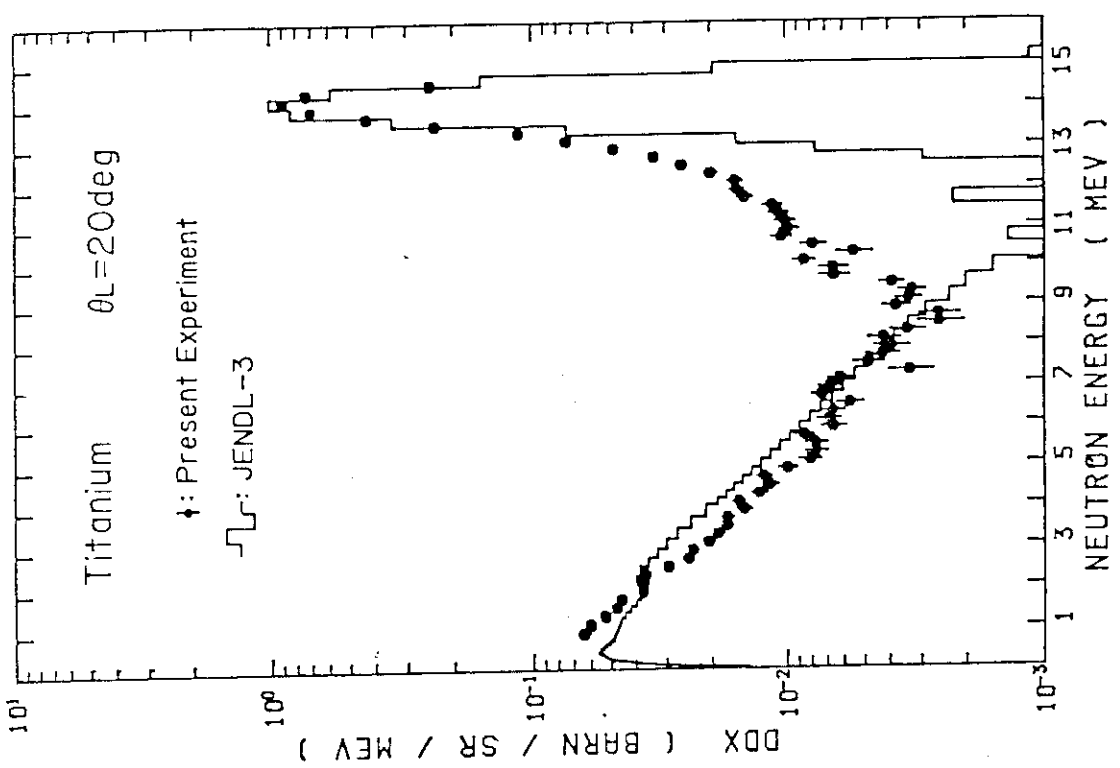


Fig.T-2 Double differential neutron emission cross sections at 20 deg, for Ti

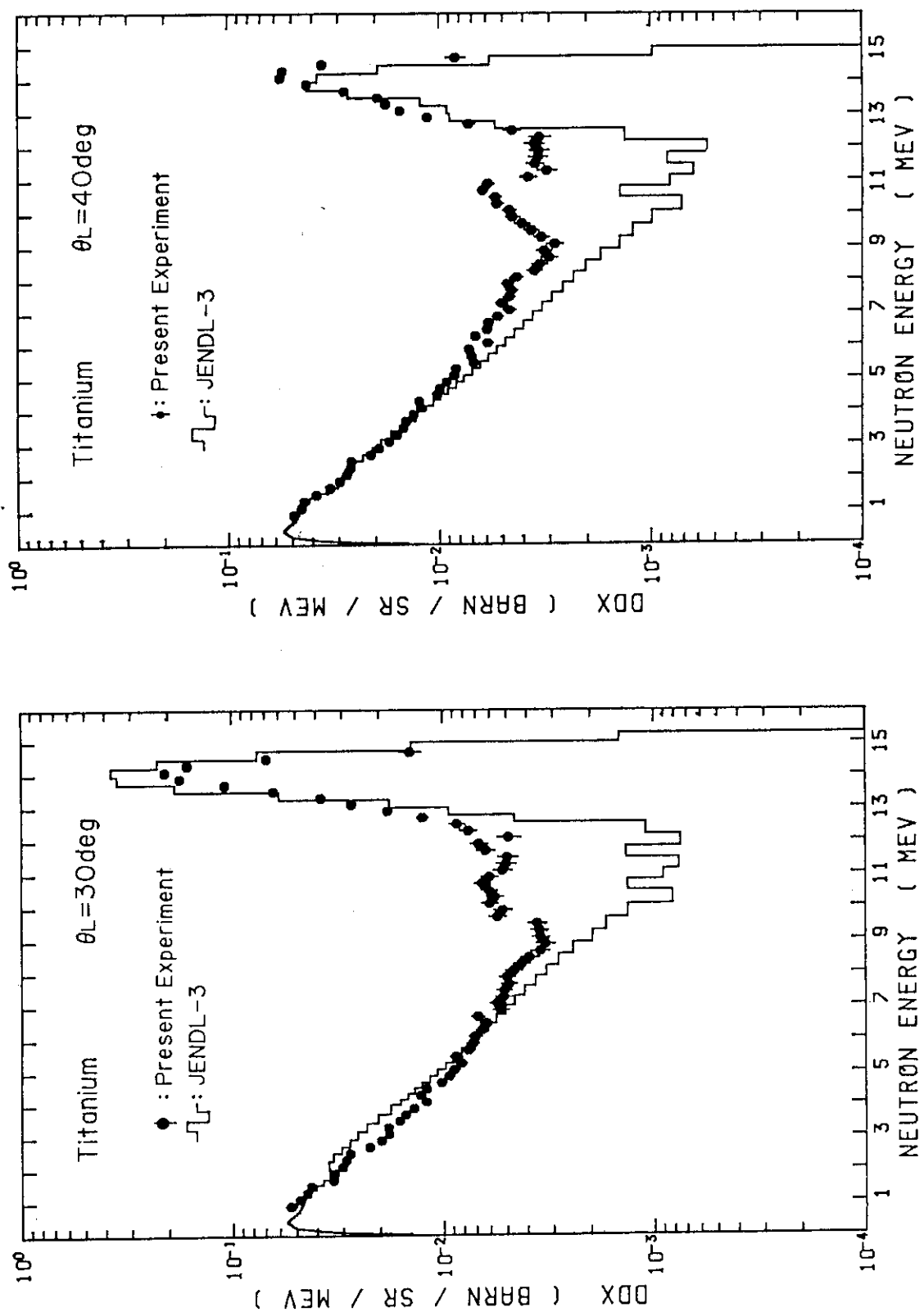


Fig.T-3 Double differential neutron emission cross sections at 30 deg, for Ti

Fig.T-4 Double differential neutron emission cross sections at 40 deg, for Ti

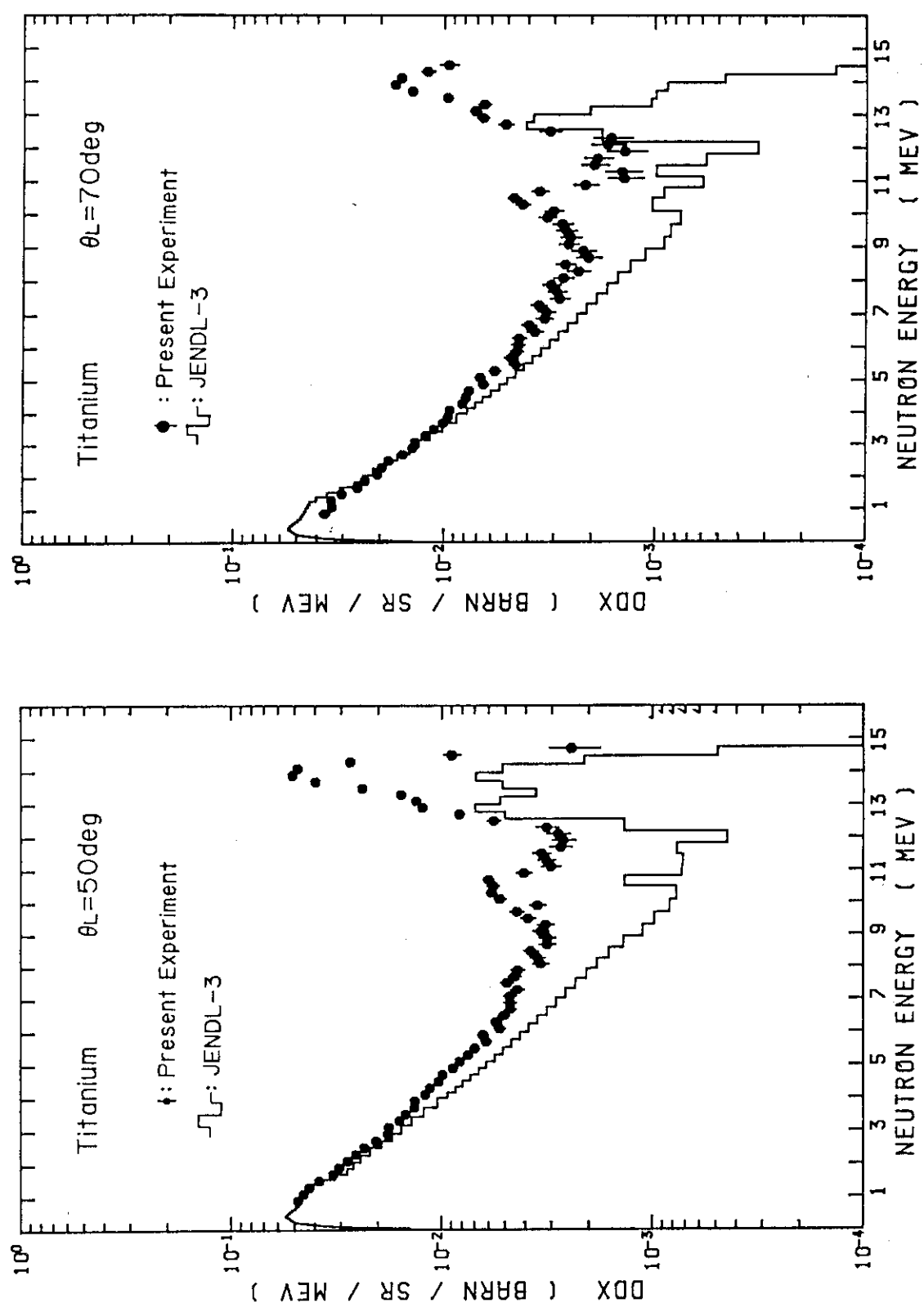


Fig.T-5 Double differential neutron emission cross sections at 50 deg, for Ti

Fig.T-6 Double differential neutron emission cross sections at 70 deg, for Ti

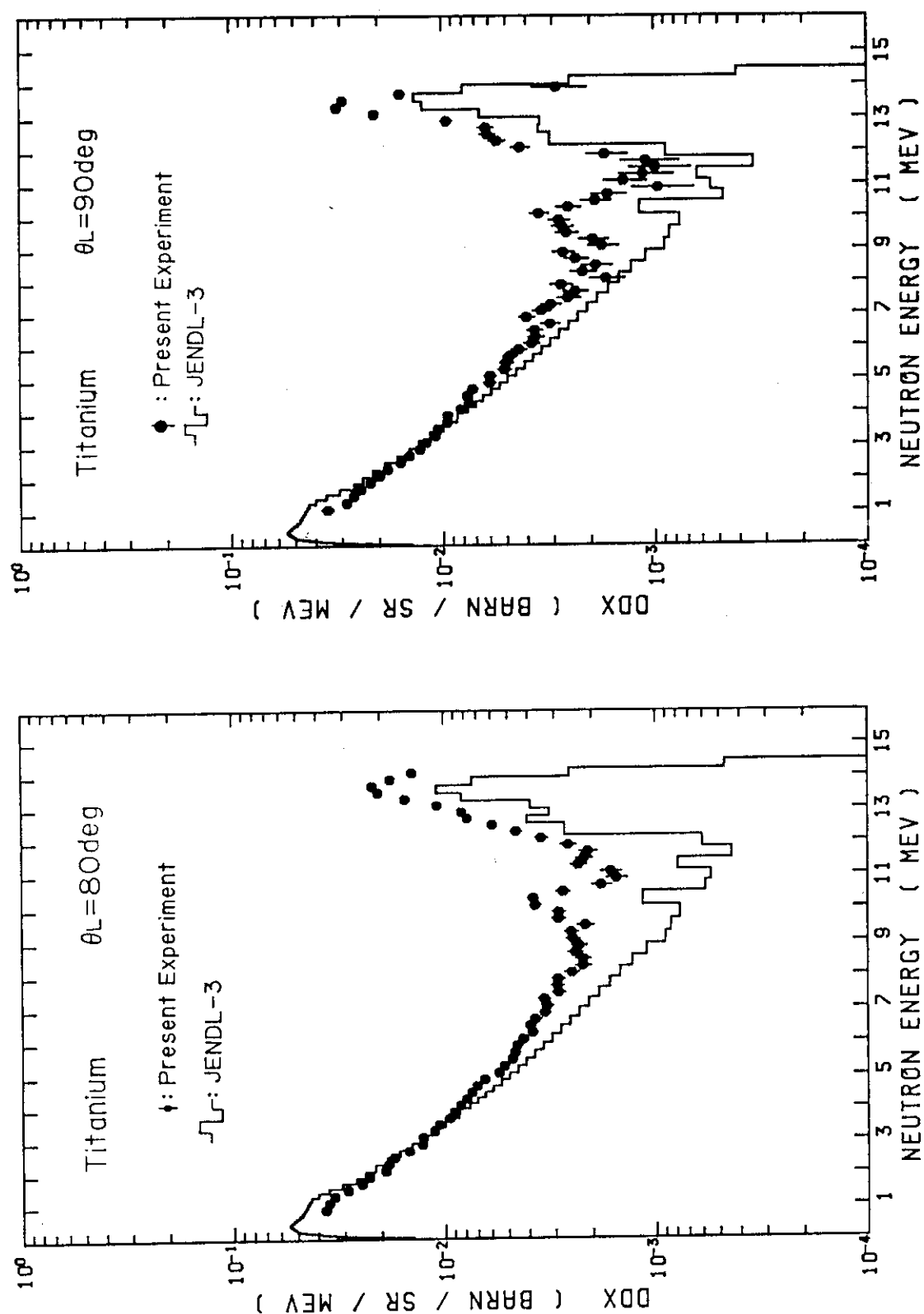


Fig.T-7 Double differential neutron emission cross sections at 80 deg, for Ti

Fig.T-8 Double differential neutron emission cross sections at 90 deg, for Ti

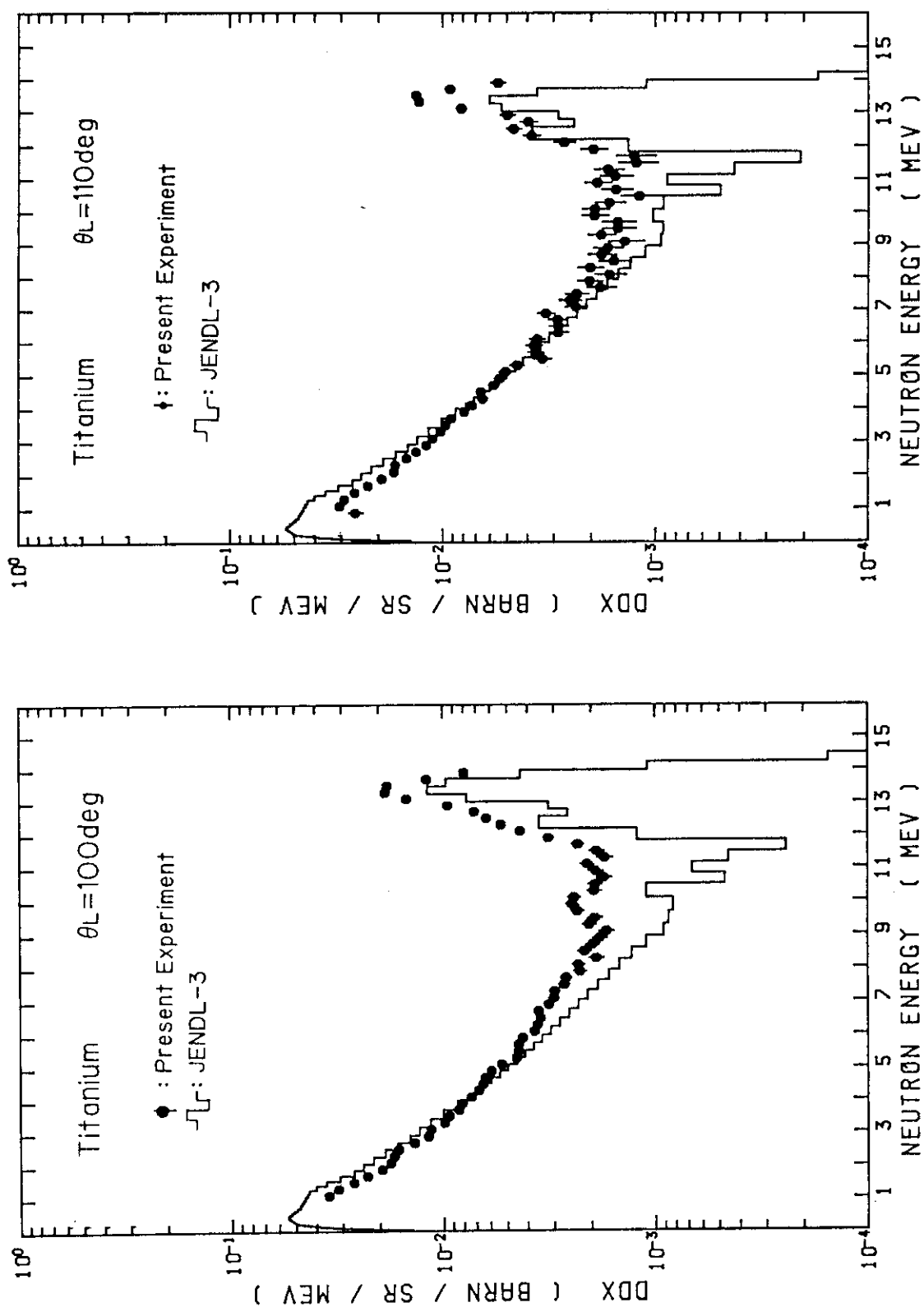


Fig.T-9 Double differential neutron emission cross sections at 100 deg, for Ti

Fig.T-10 Double differential neutron emission cross sections at 110 deg, for Ti

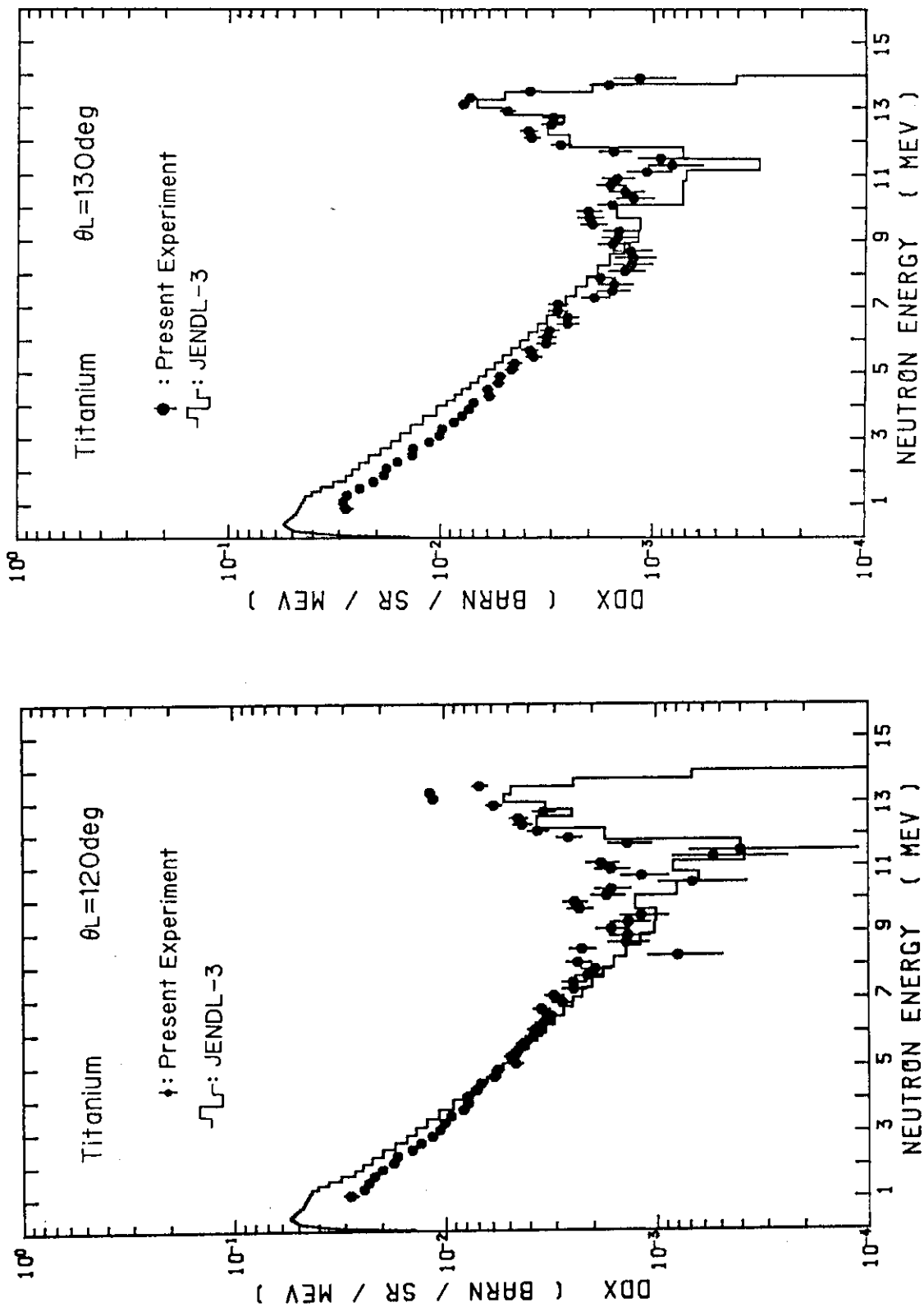


Fig.T-11 Double differential neutron emission cross sections at 120 deg, for Ti

Fig.T-12 Double differential neutron emission cross sections at 130 deg, for Ti

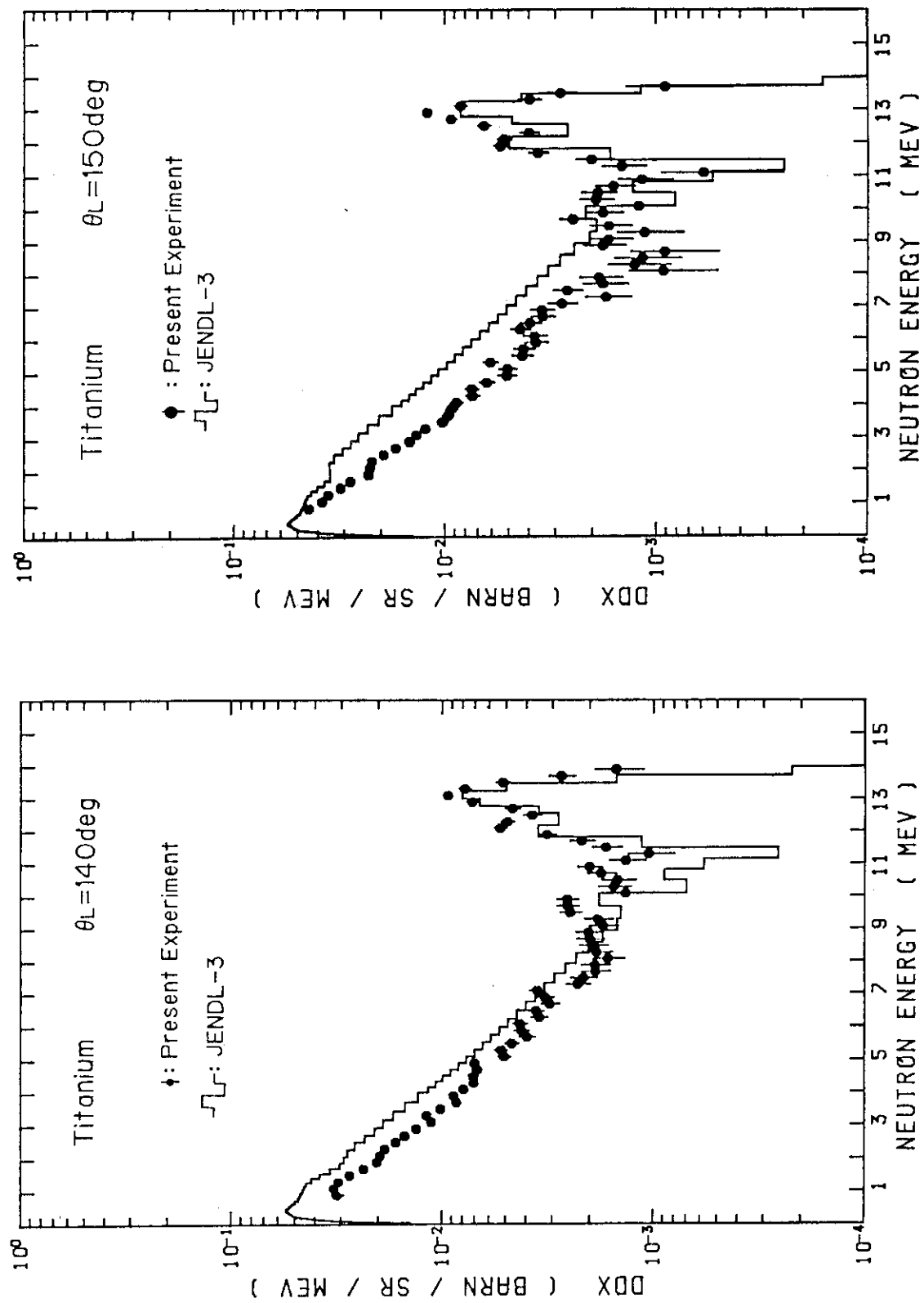


Fig.T-13 Double differential neutron emission cross sections at 140 deg, for Ti

Fig.T-14 Double differential neutron emission cross sections at 150 deg, for Ti

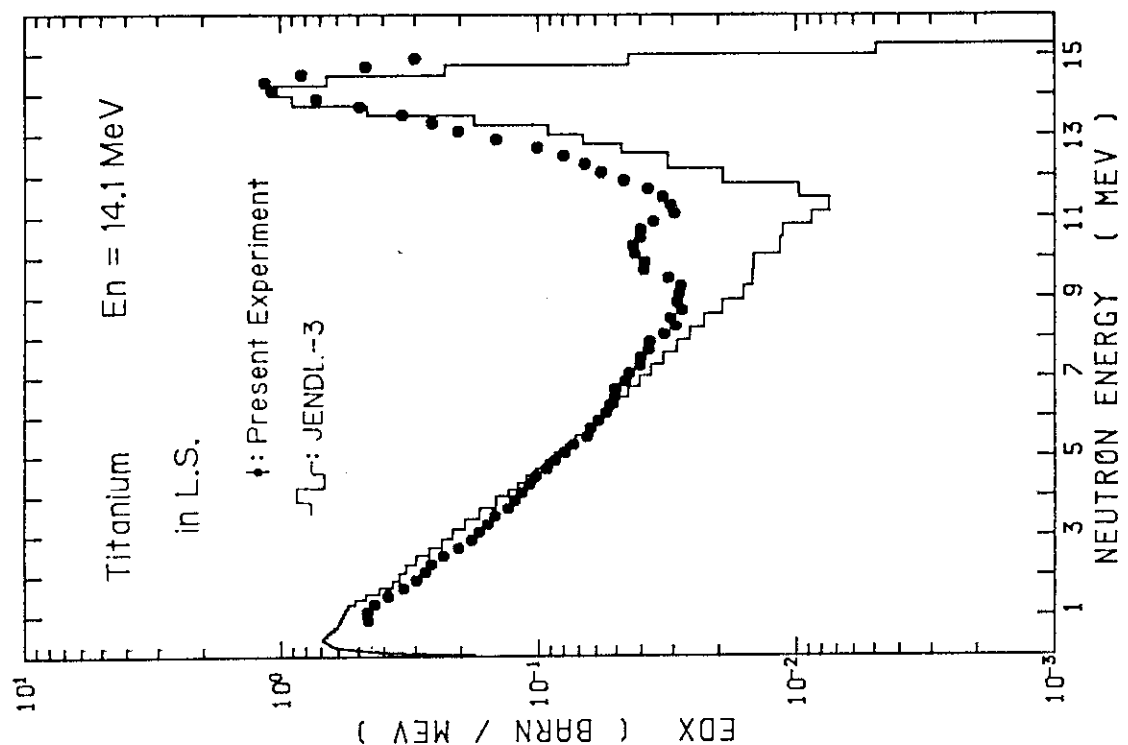


Fig.T-16 Angle-integrated neutron emission spectra in LAB system, for Ti

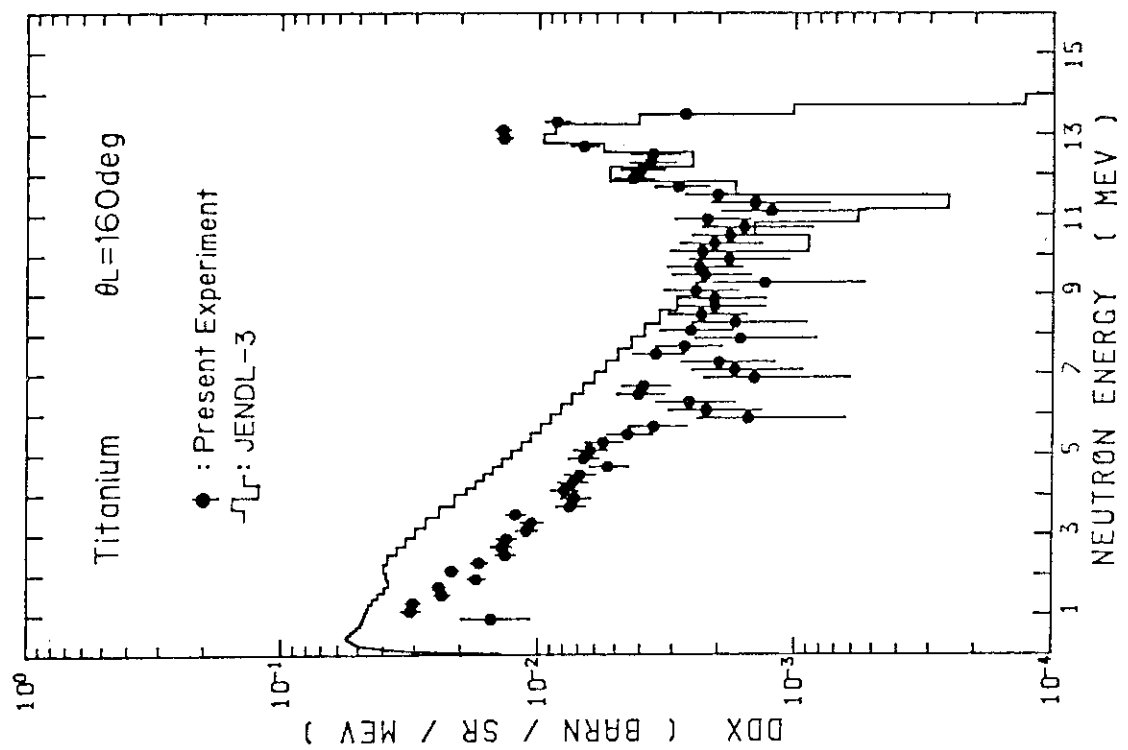


Fig.T-15 Double differential neutron emission cross sections at 160 deg , for Ti

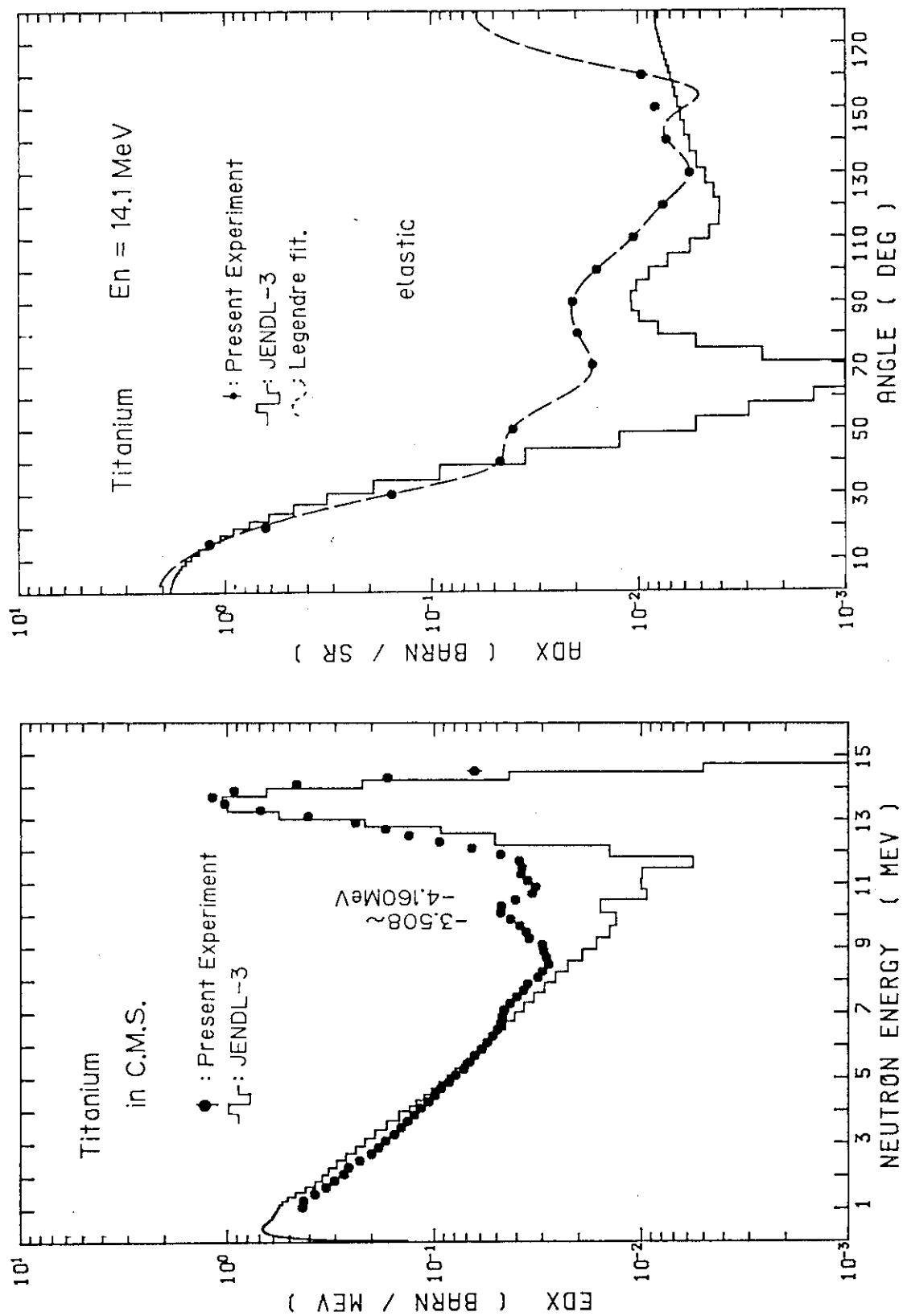


Fig.T-17 Angle-integrated neutron emission spectra in CMS, for Ti

Fig.T-18 Differential elastic scattering cross sections, for Ti

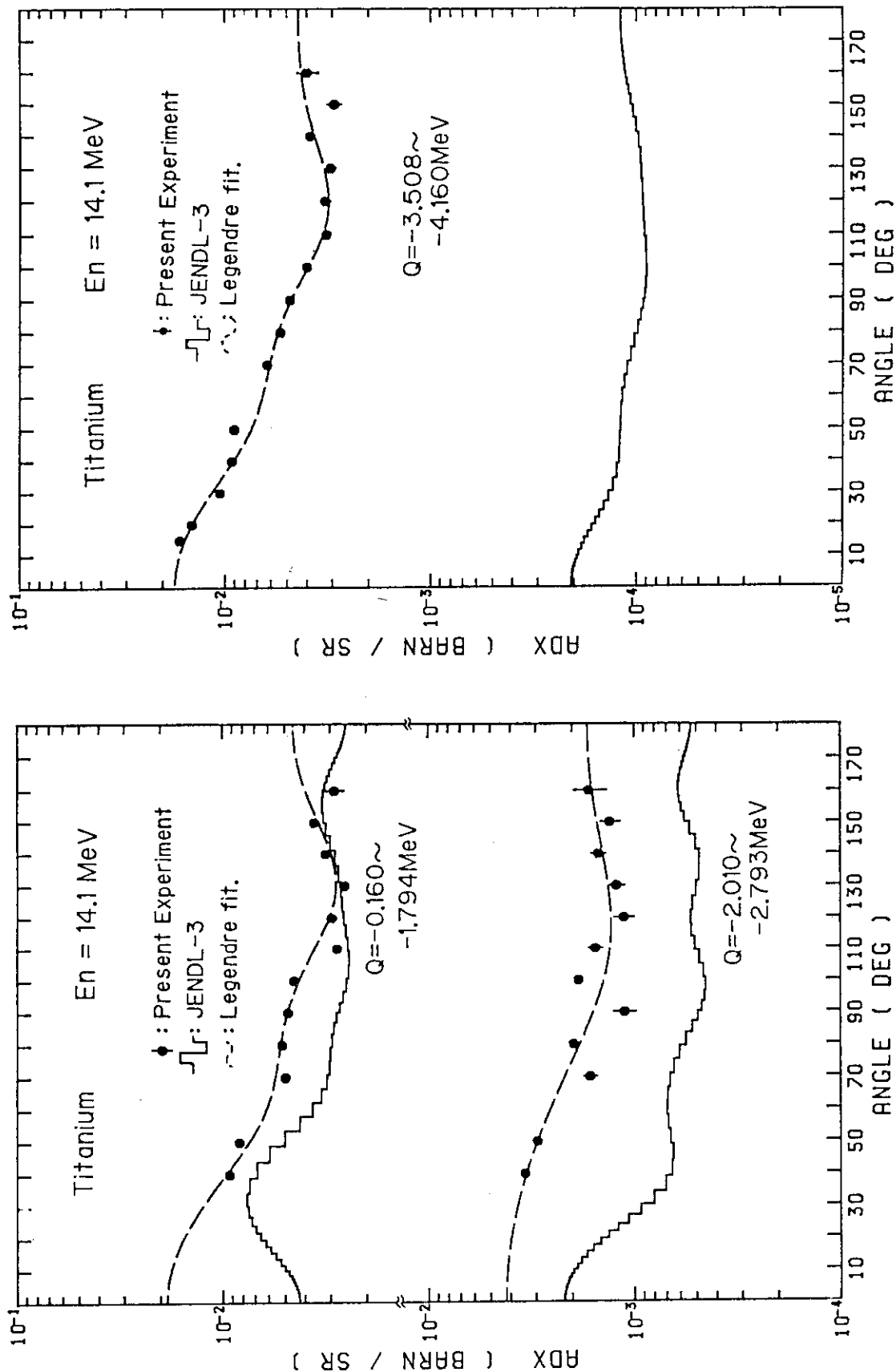


Fig.T-19 Differential inelastic scattering cross sections, for Ti

Fig.T-20 Differential inelastic scattering cross sections, for Ti

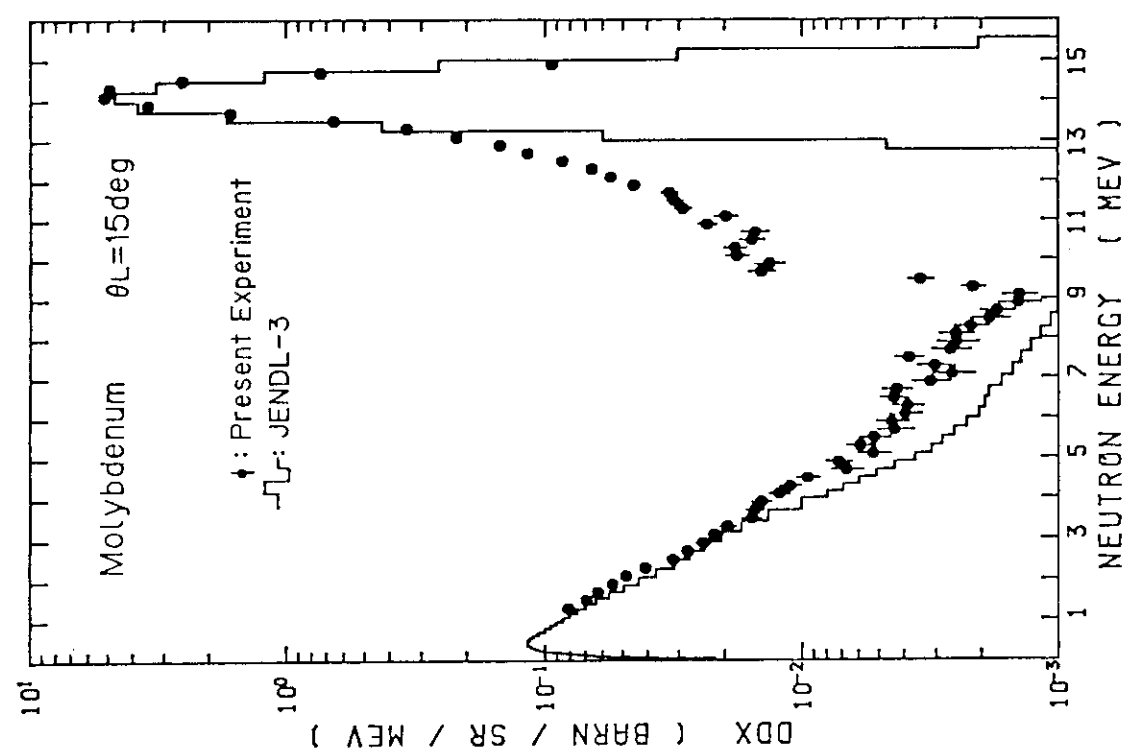


Fig.M-1 Double differential neutron emission cross sections at 15 deg, for Mo

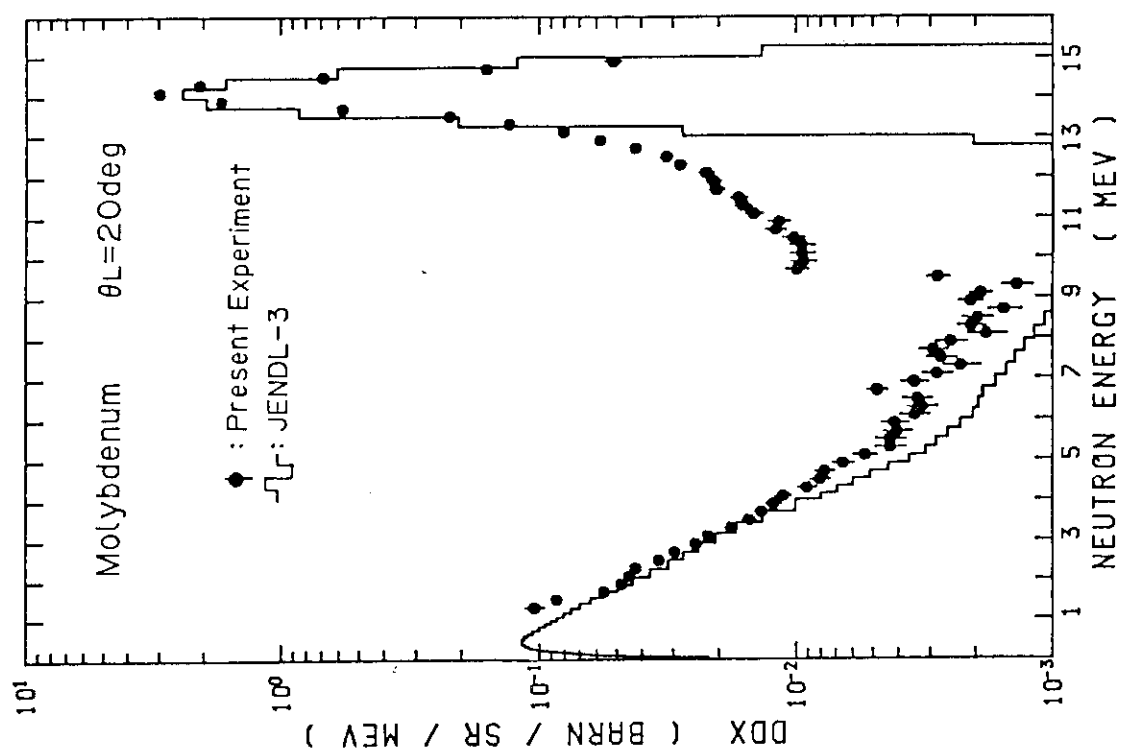


Fig.M-2 Double differential neutron emission cross sections at 20 deg, for Mo

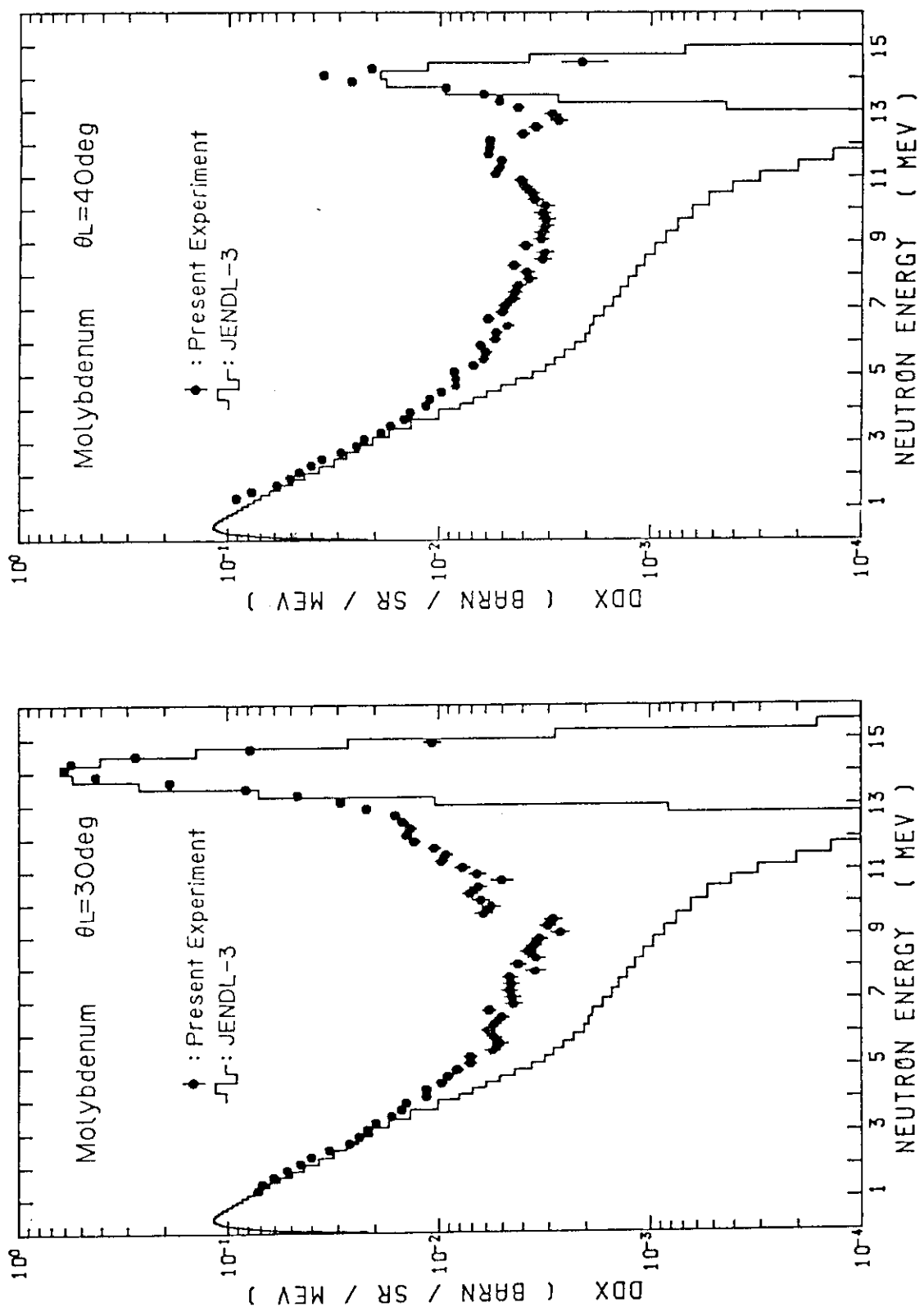


Fig.M-3 Double differential neutron emission cross sections at 30 deg, for Mo

Fig.M-4 Double differential neutron emission cross sections at 40 deg, for Mo

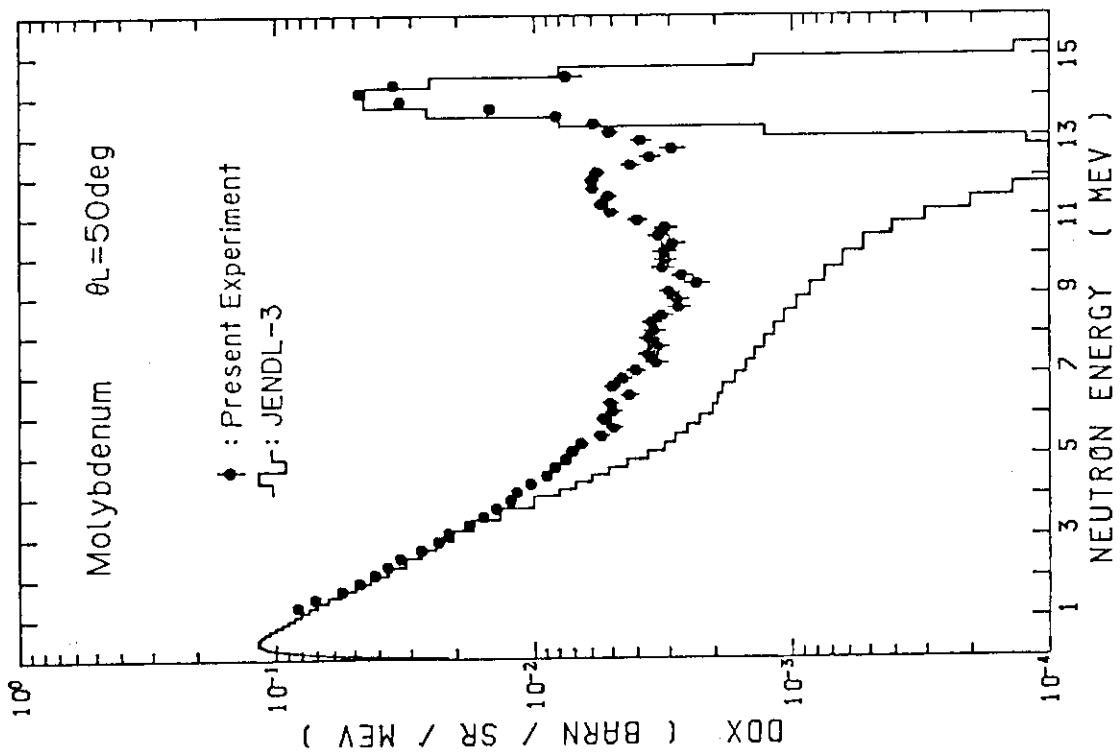


Fig.M-5 Double differential neutron emission cross sections at 50 deg, for Mo

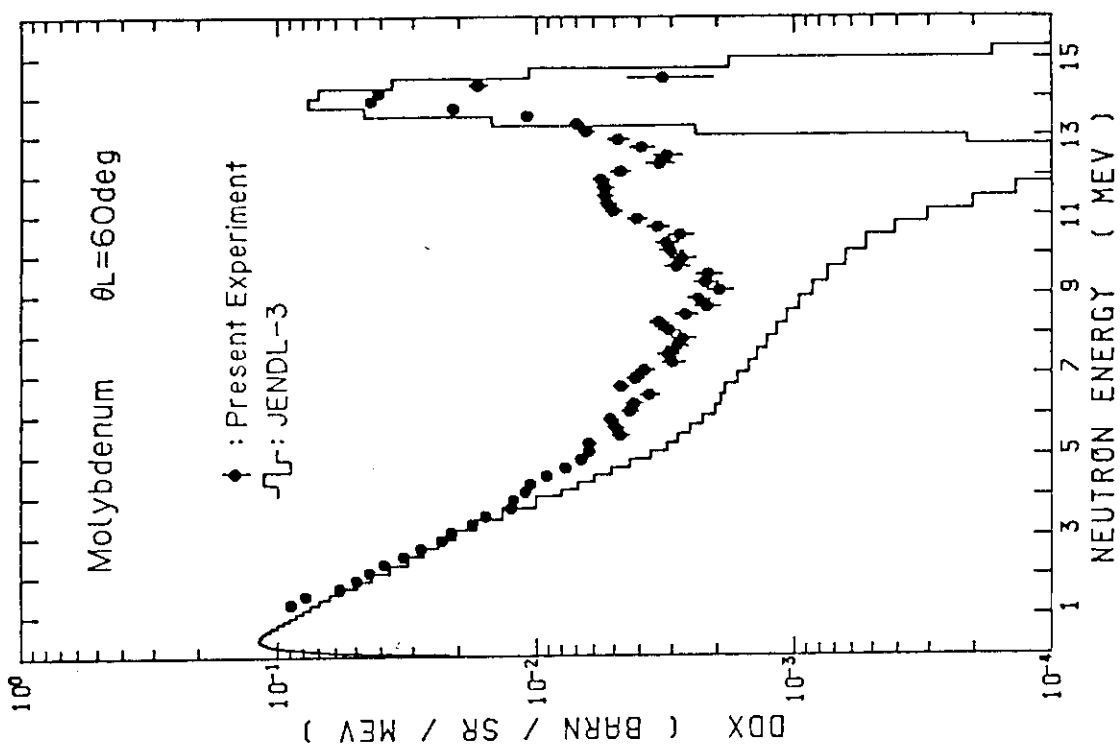


Fig.M-6 Double differential neutron emission cross sections at 60 deg, for Mo

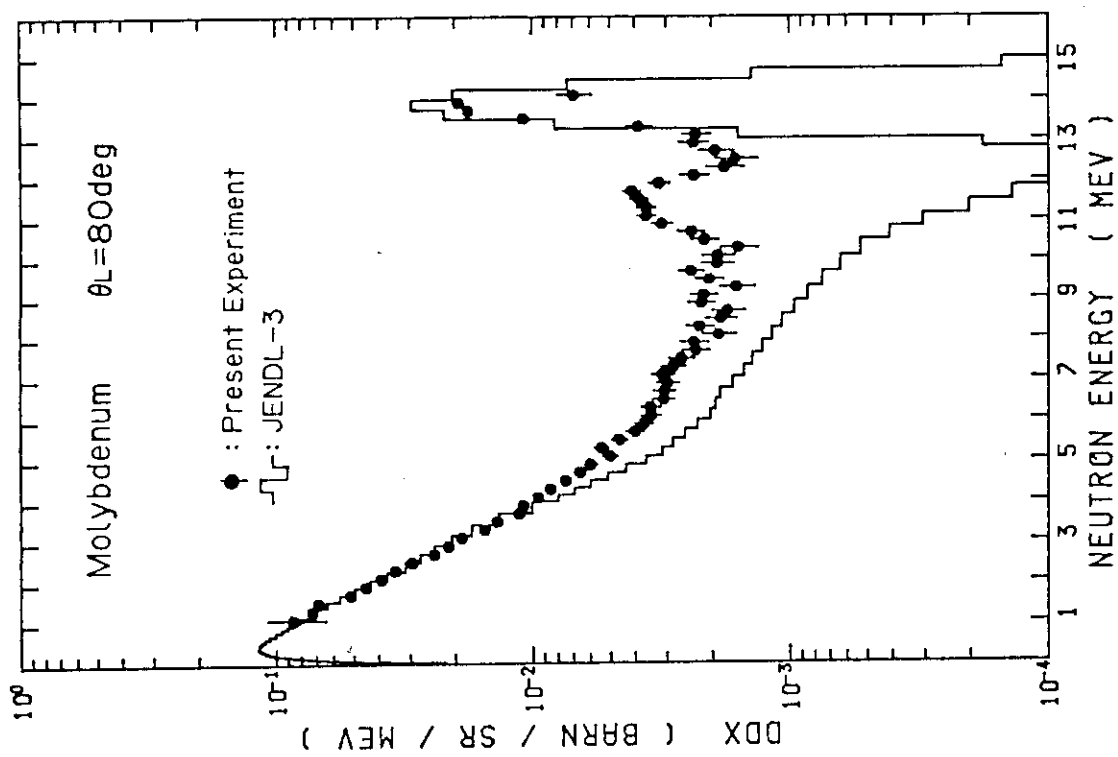
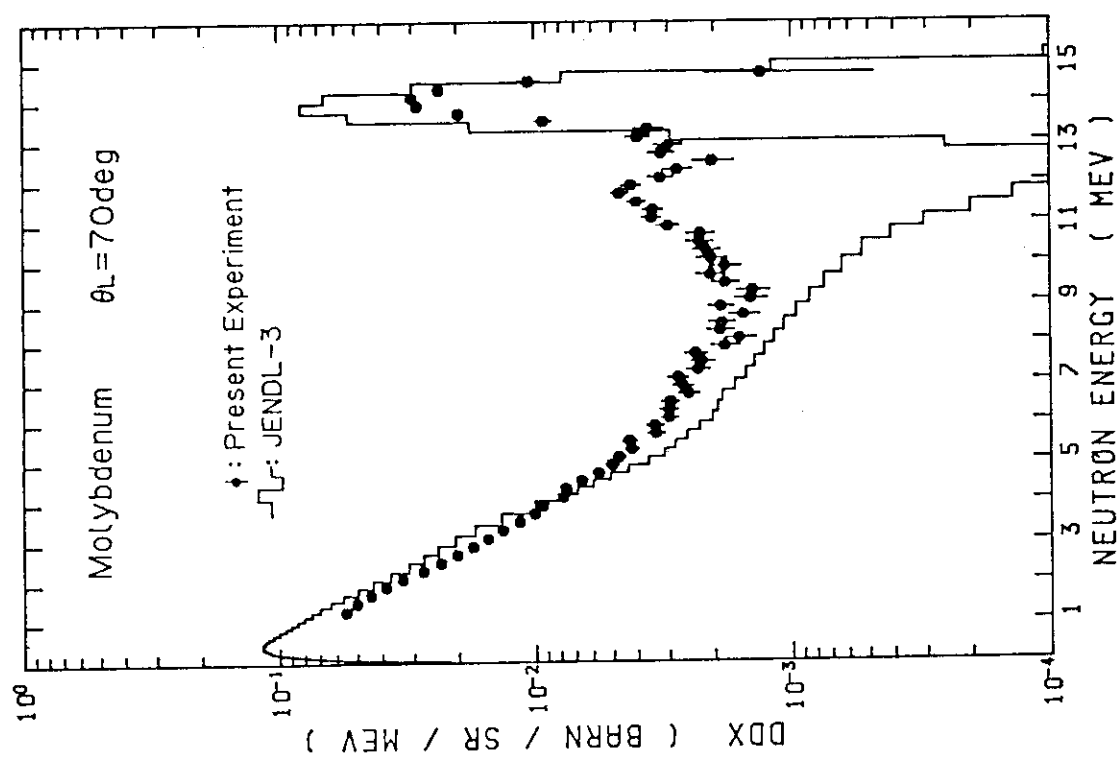


Fig.M-7 Double differential neutron emission cross sections at 70 deg, for Mo

Fig.M-8 Double differential neutron emission cross sections at 80 deg, for Mo

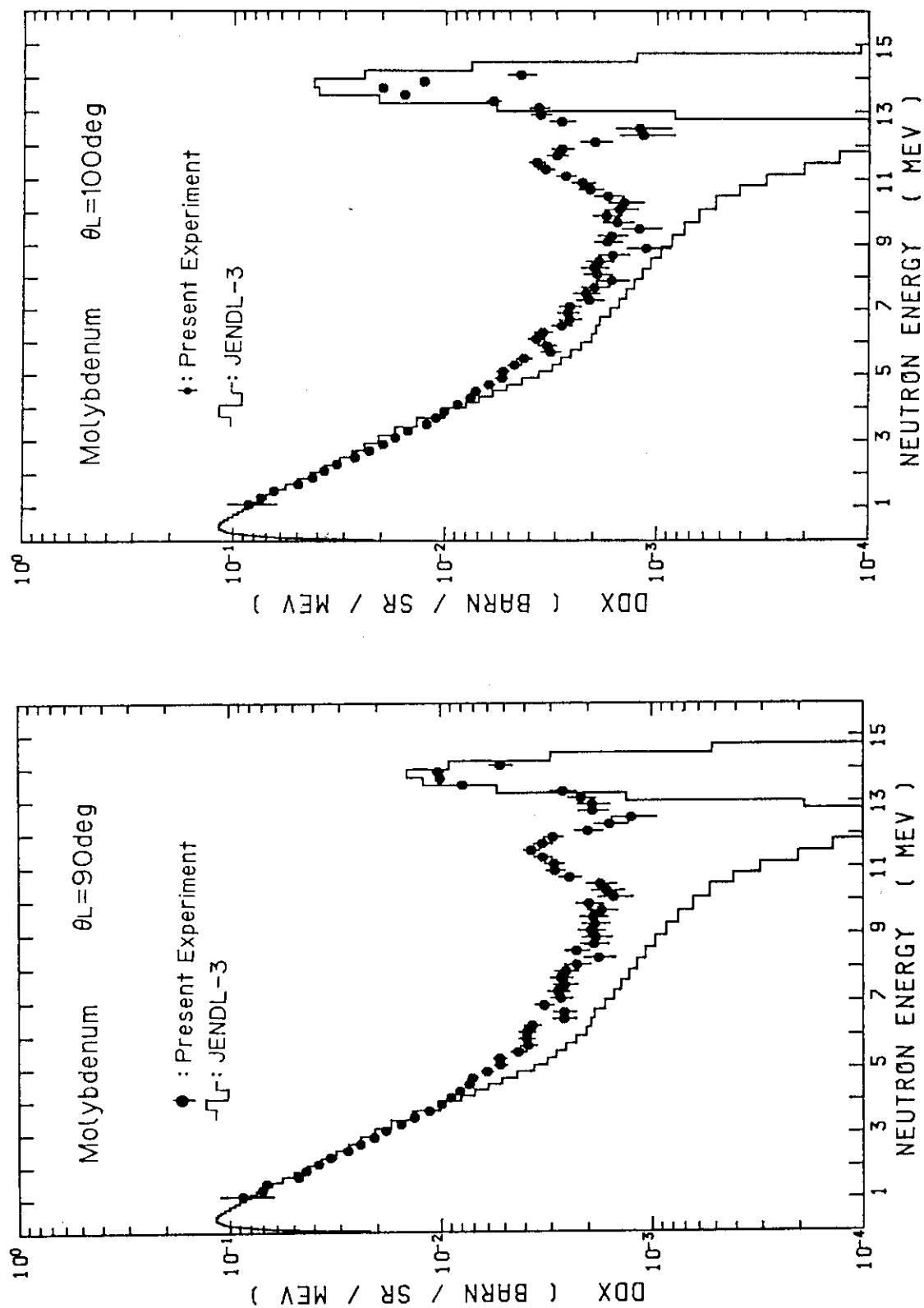


Fig.M-9 Double differential neutron emission cross sections at 90 deg, for Mo

Fig.M-10 Double differential neutron emission cross sections at 100 deg, for Mo

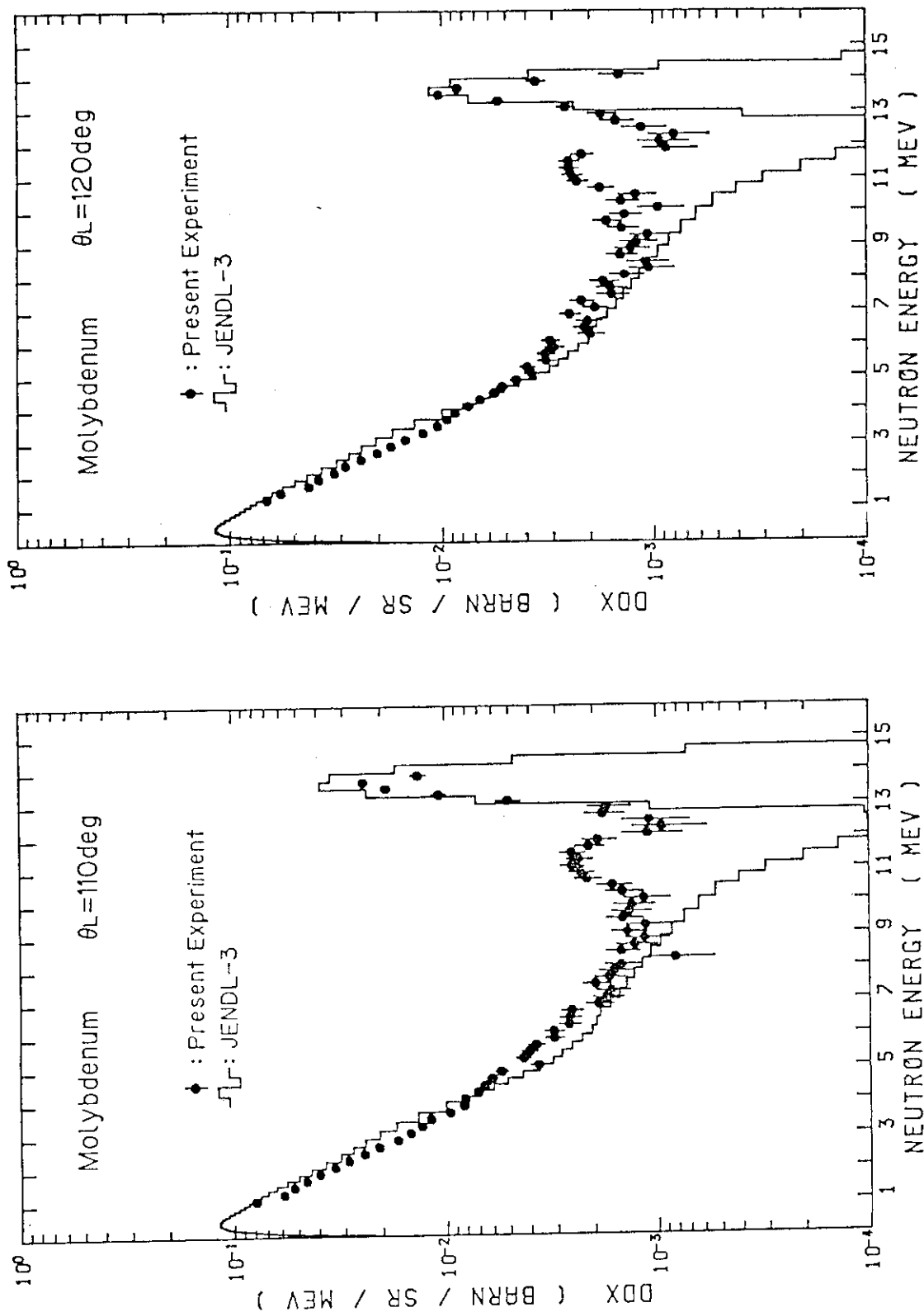


Fig.M-11 Double differential neutron emission cross sections at 110 deg, for Mo
Fig.M-12 Double differential neutron emission cross sections at 120 deg, for Mo

Fig.M-11 Double differential neutron emission cross sections at 110 deg, for Mo
Fig.M-12 Double differential neutron emission cross sections at 120 deg, for Mo

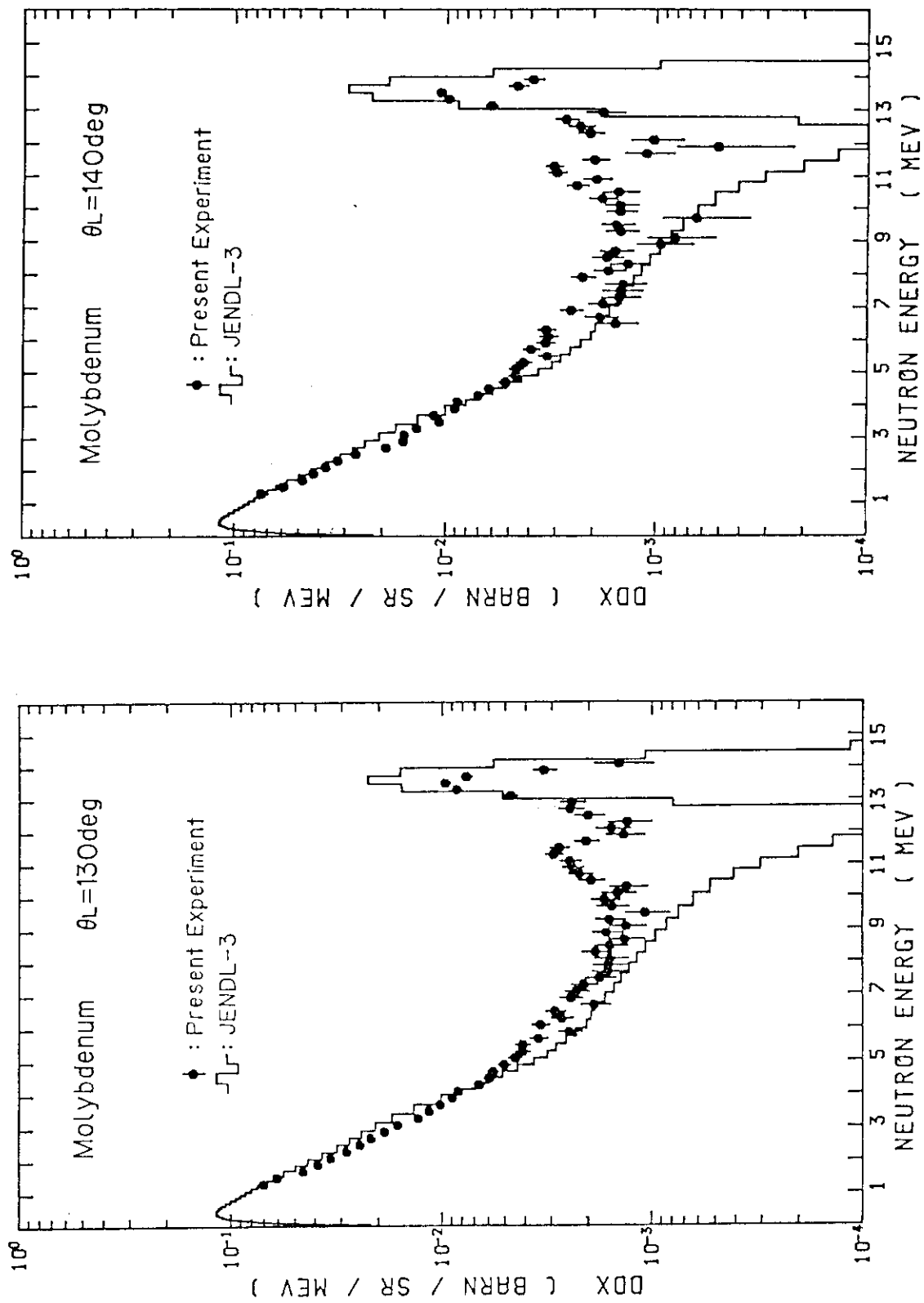


Fig.M-13 Double differential neutron emission cross sections at 130 deg, for Mo Fig.M-14 Double differential neutron emission cross sections at 140 deg, for Mo

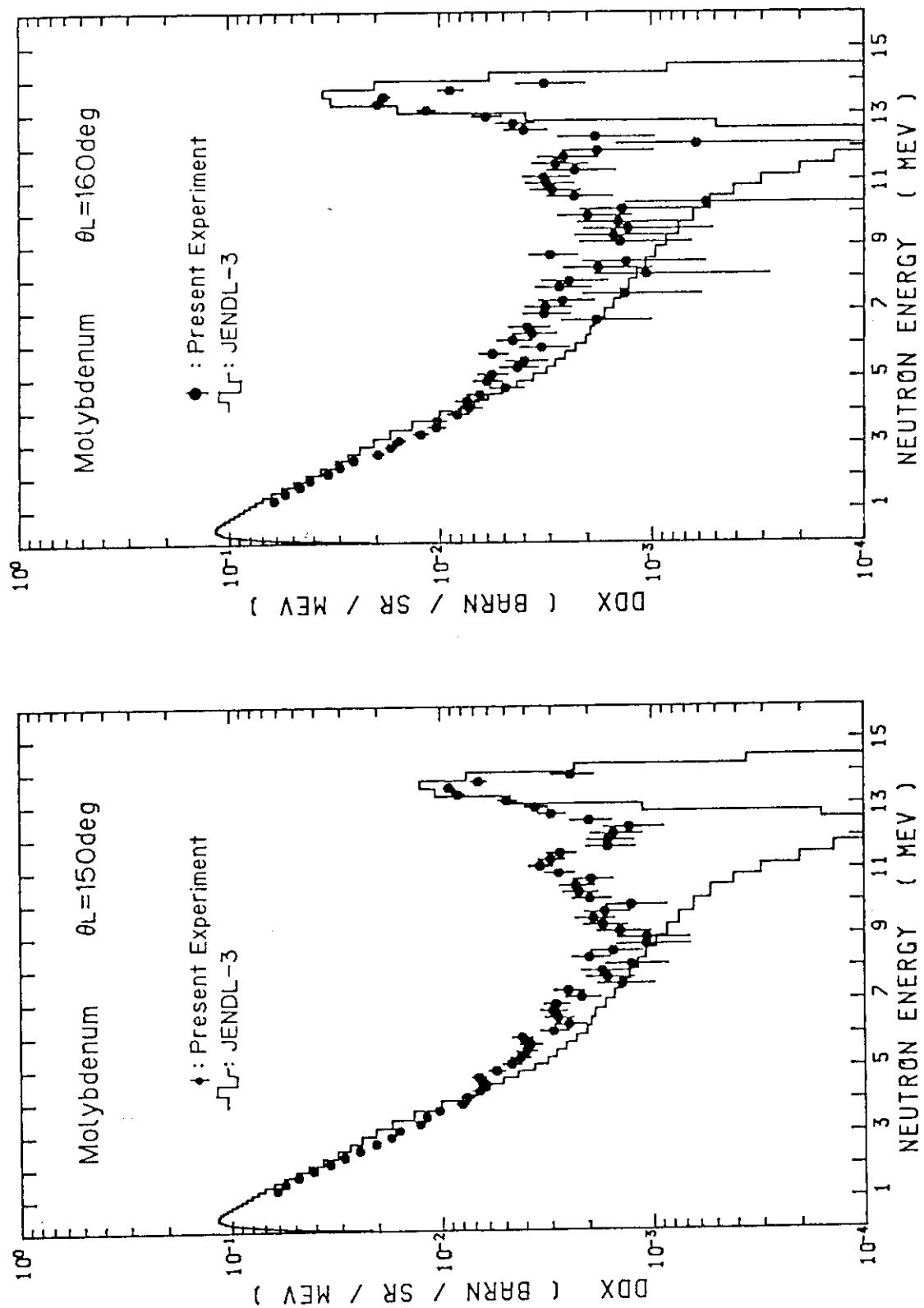


Fig.M-15 Double differential neutron emission cross sections at 160 deg, for Mo
Fig.M-16 Double differential neutron emission cross sections at 150 deg, for Mo

Fig.M-15 Double differential neutron emission cross sections at 150 deg, for Mo
Fig.M-16 Double differential neutron emission cross sections at 160 deg, for Mo

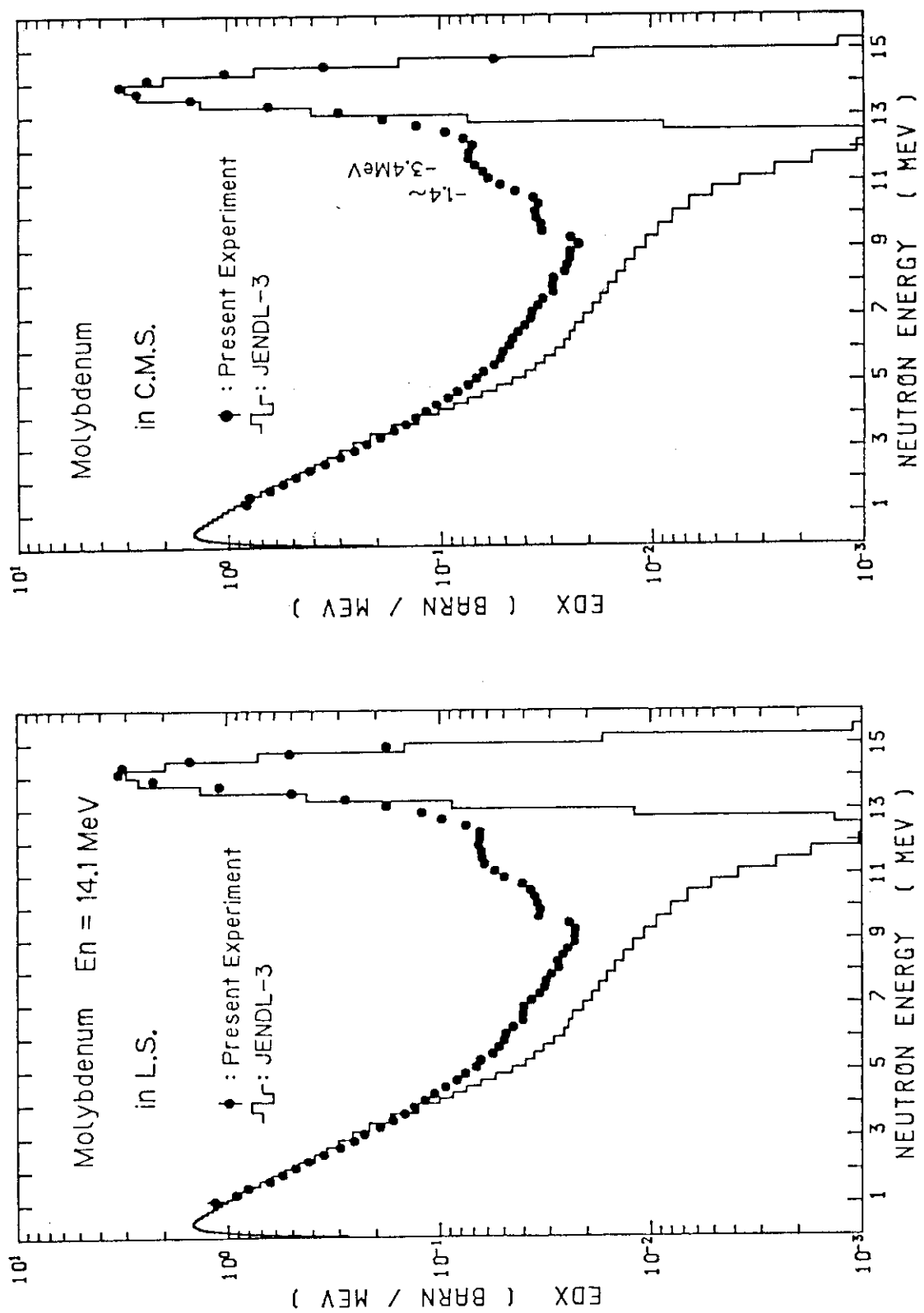


Fig.M-17 Angle-integrated neutron emission spectra in LAB system, for Mo

Fig.M-18 Angle-integrated neutron emission spectra in CMS, for Mo

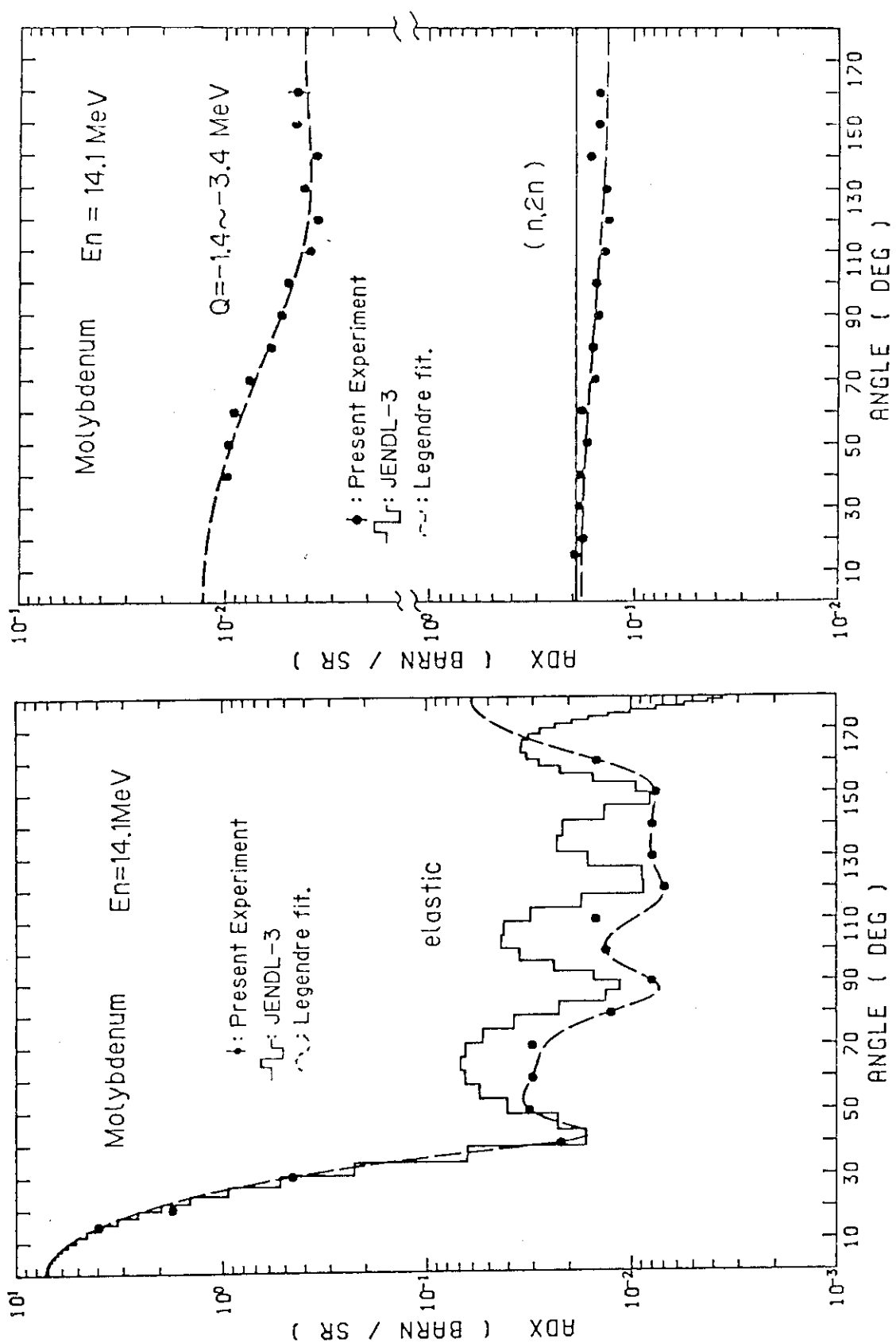


Fig.M-19 Differential elastic scattering cross sections, for Mo

Fig.M-20 Differential cross sections of inelastic scattering (upper) and $(n, 2n)$ reaction (lower), for Mo

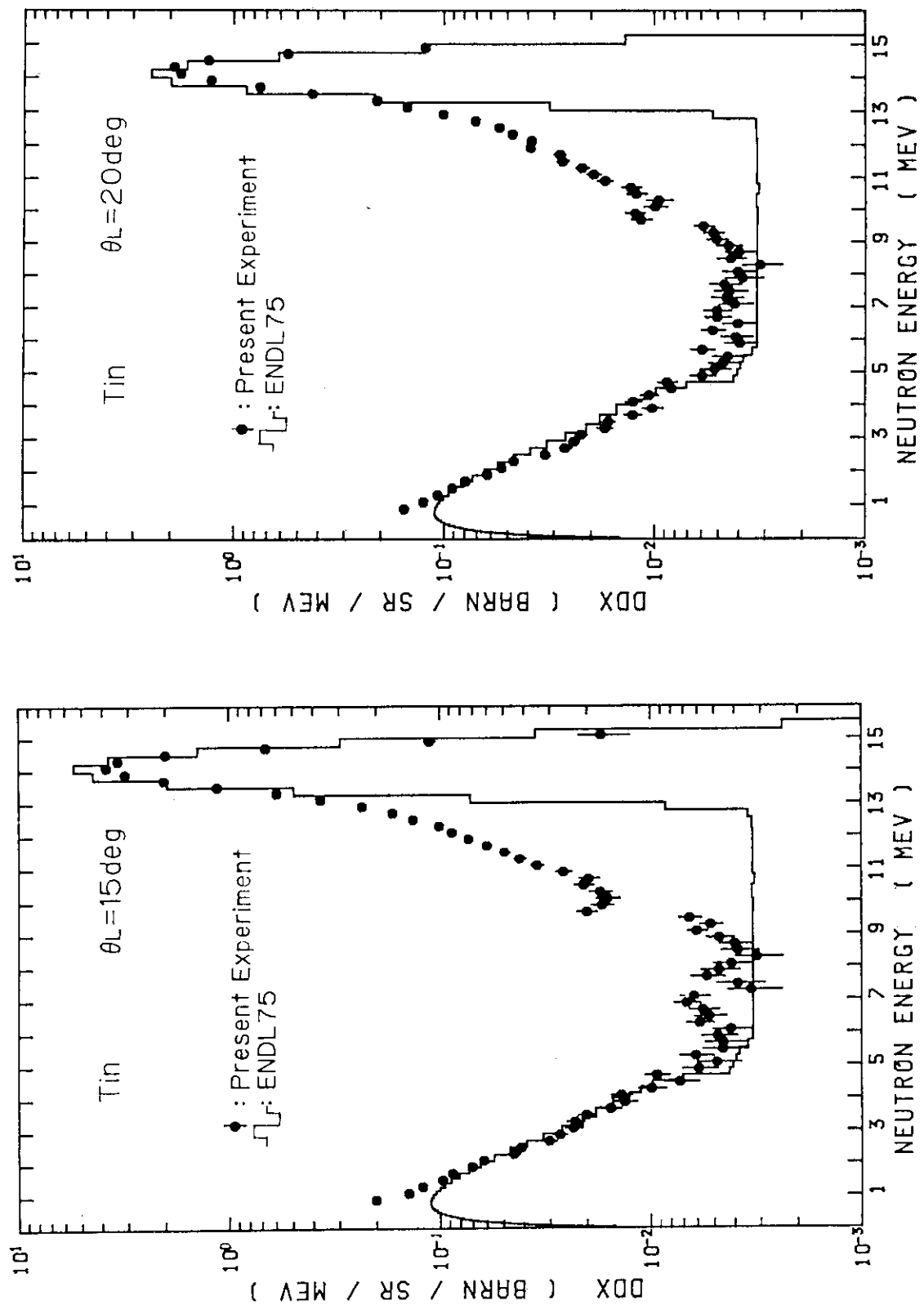


Fig.S-1 Double differential neutron emission cross sections at 15 deg, for Sn

Fig.S-2 Double differential neutron emission cross sections at 20 deg, for Sn

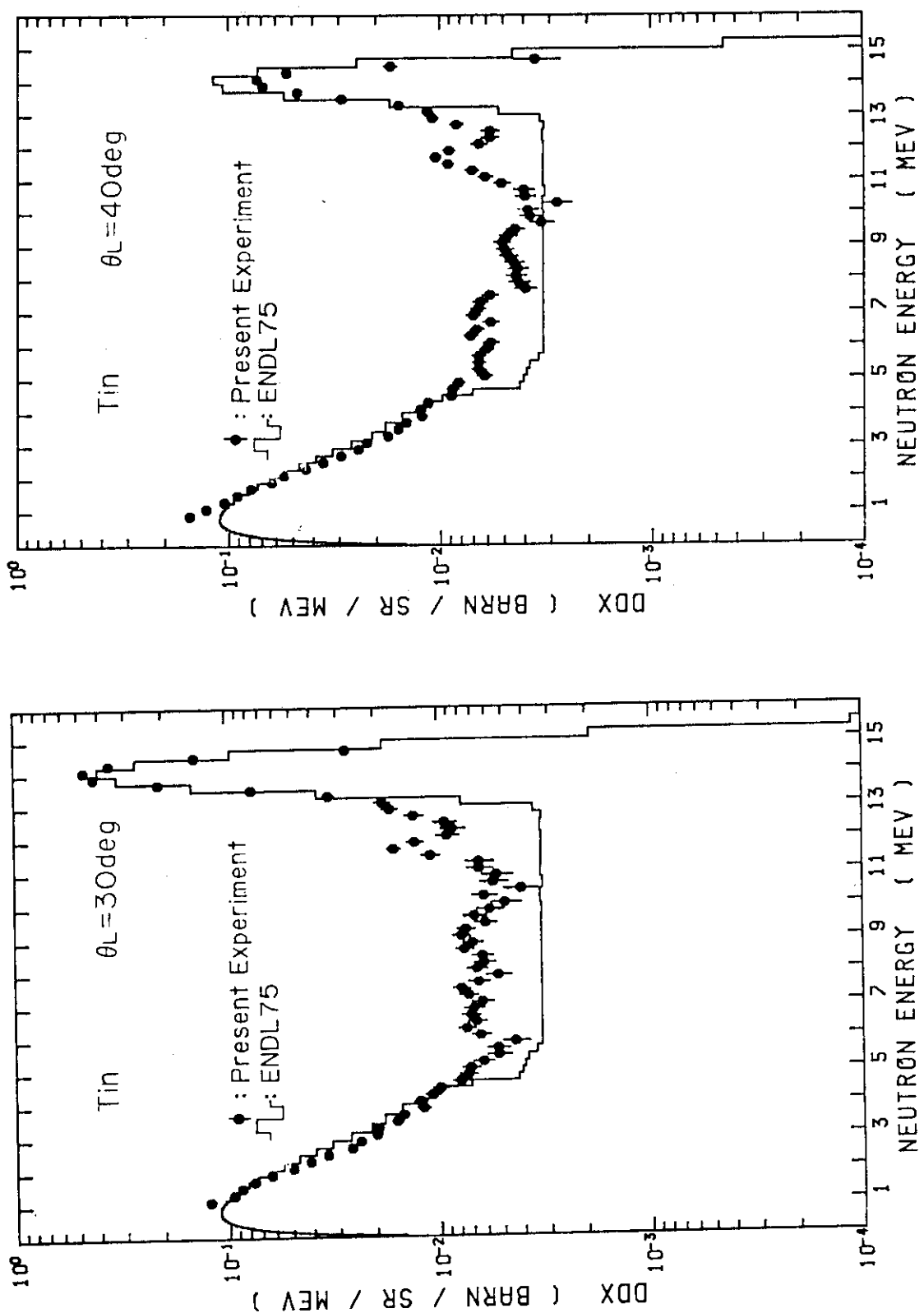


Fig.S-3 Double differential neutron emission cross sections at 30 deg, for Sn

Fig.S-4 Double differential neutron emission cross sections at 40 deg, for Sn

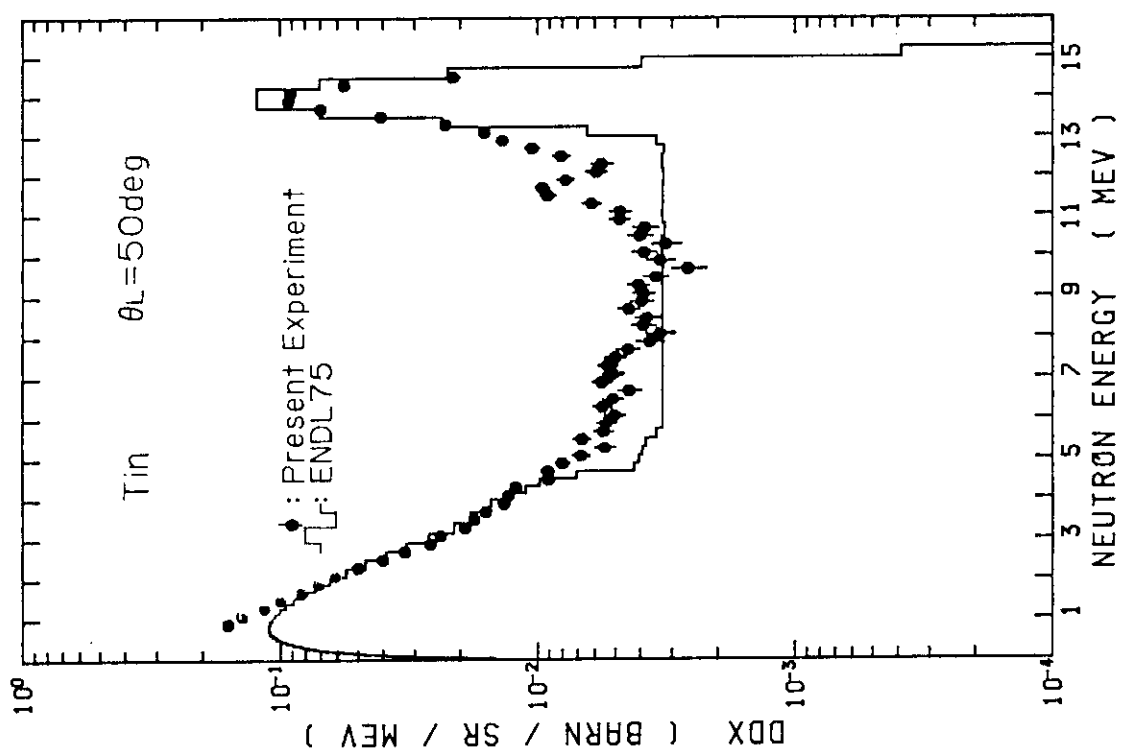


Fig.S-5 Double differential neutron emission cross sections at 50 deg, for Sn

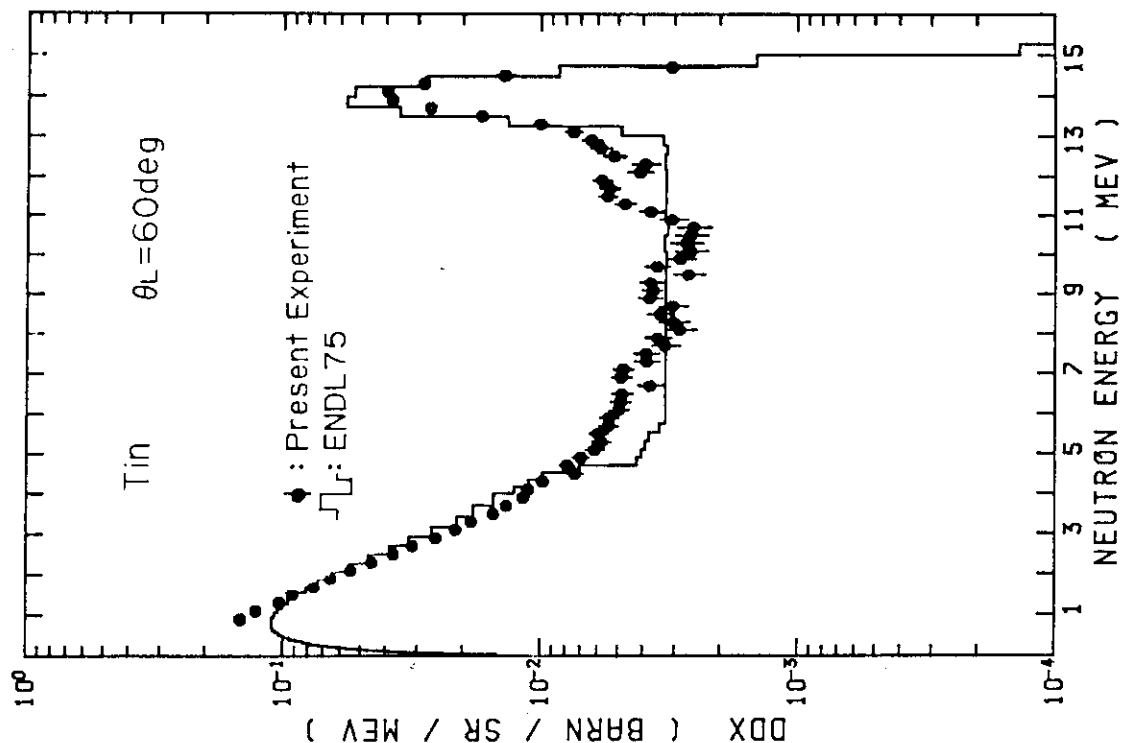


Fig.S-6 Double differential neutron emission cross sections at 60 deg, for Sn

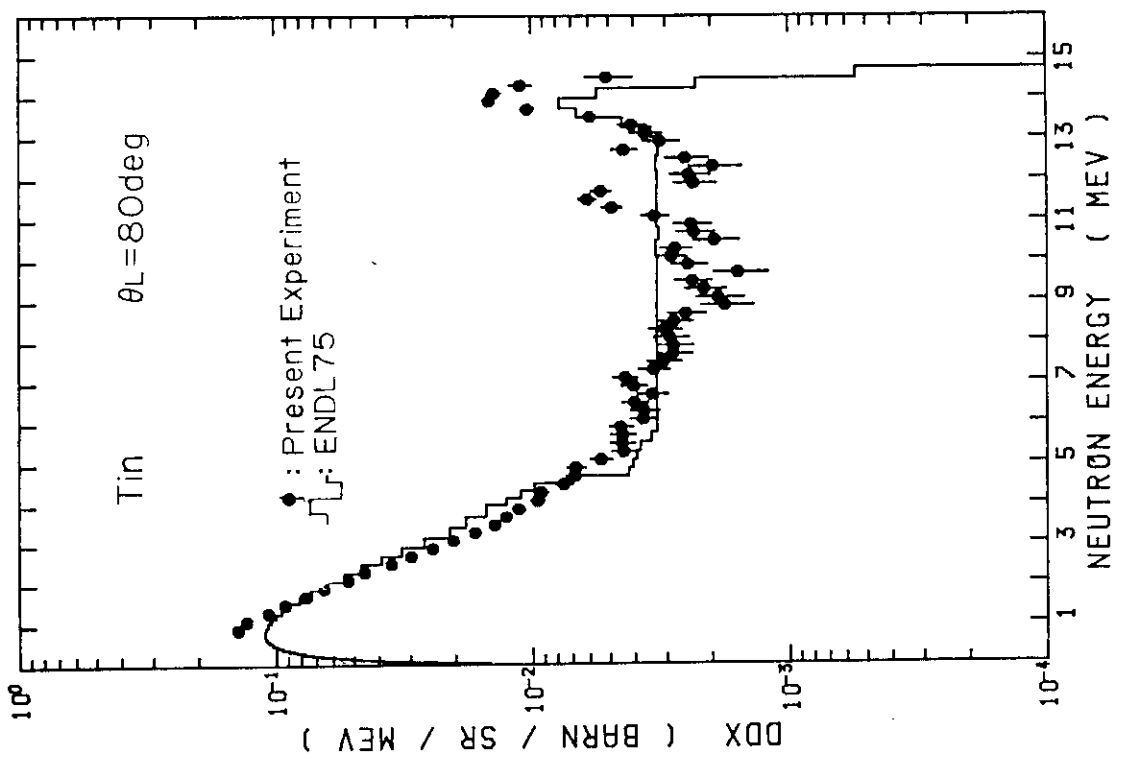
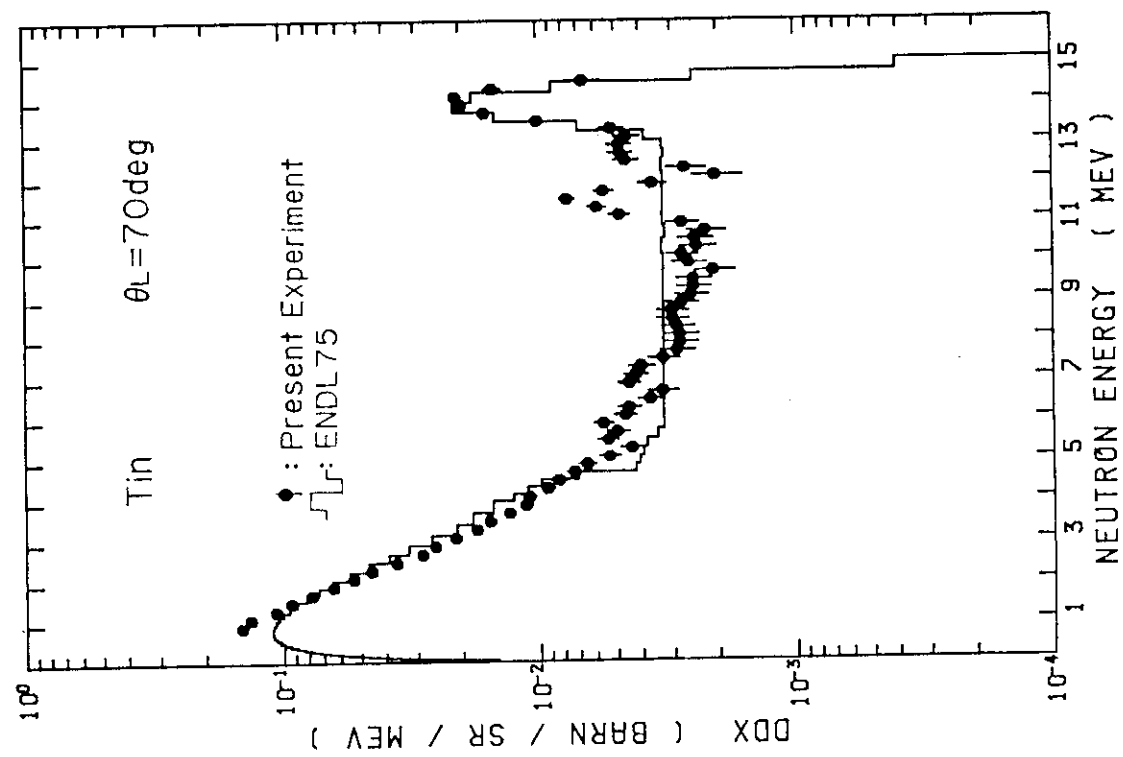


Fig.S-7 Double differential neutron emission cross sections at 70 deg, for Sn

Fig.S-8 Double differential neutron emission cross sections at 80 deg, for Sn

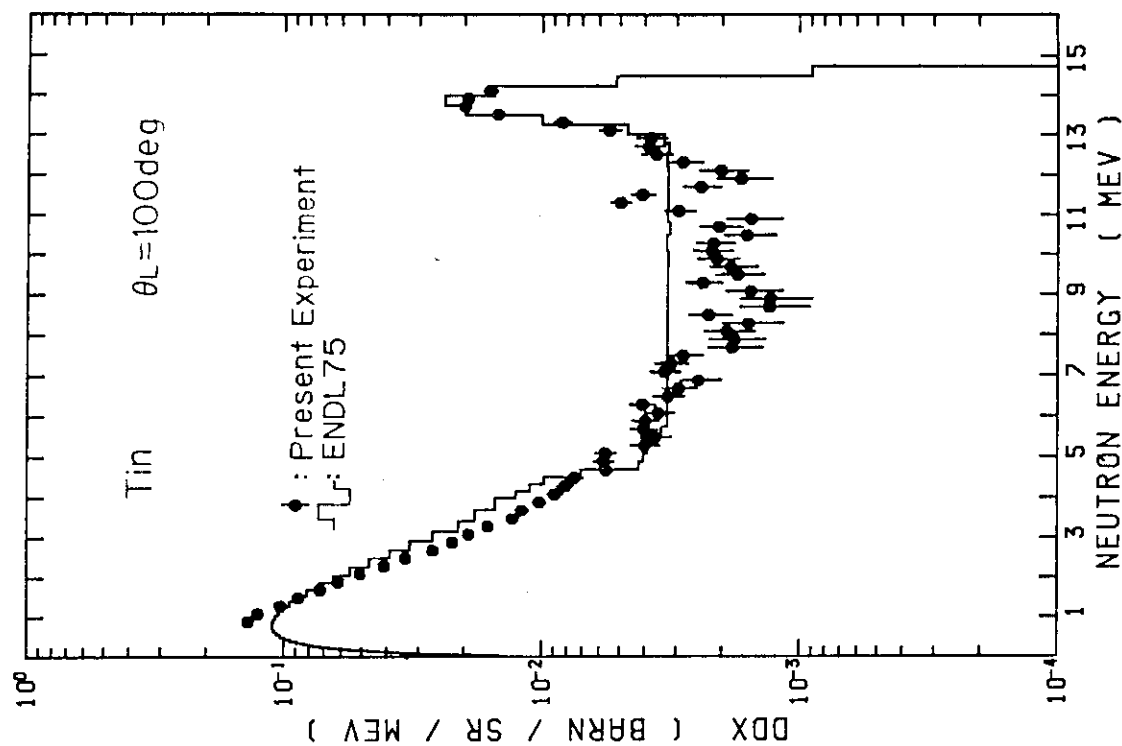
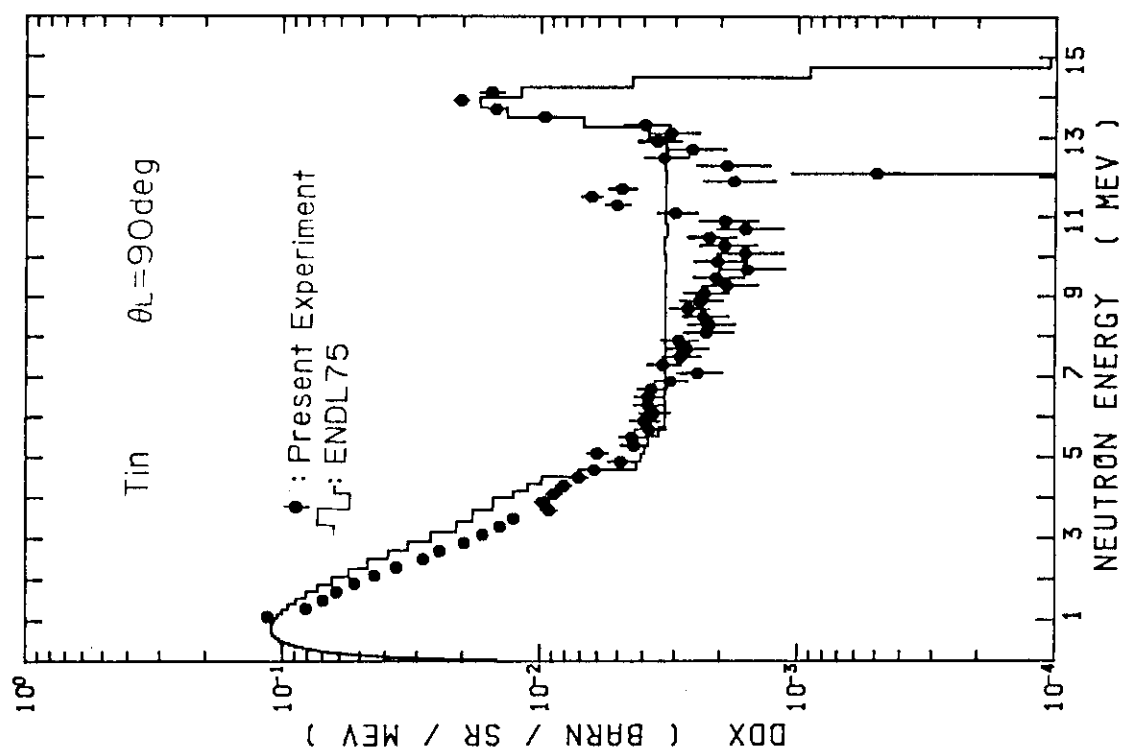


Fig.S-9 Double differential neutron emission cross sections at 90 deg, for Sn

Fig.S-10 Double differential neutron emission cross sections at 100 deg, for Sn

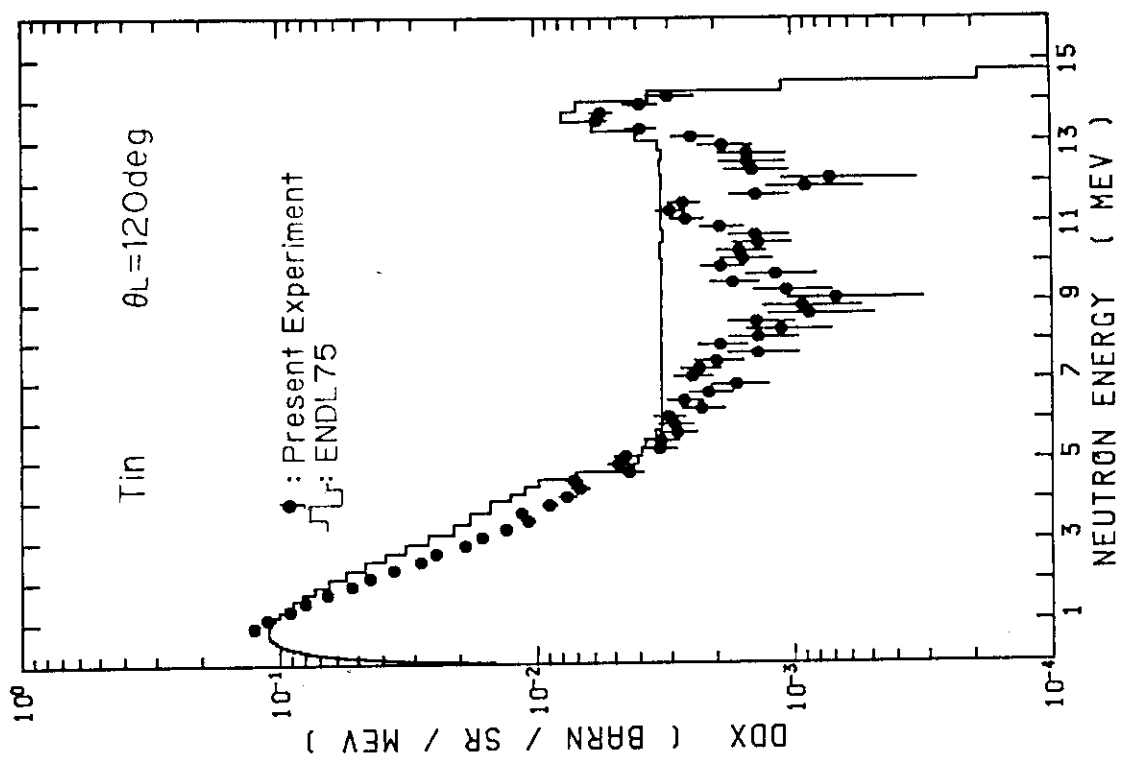
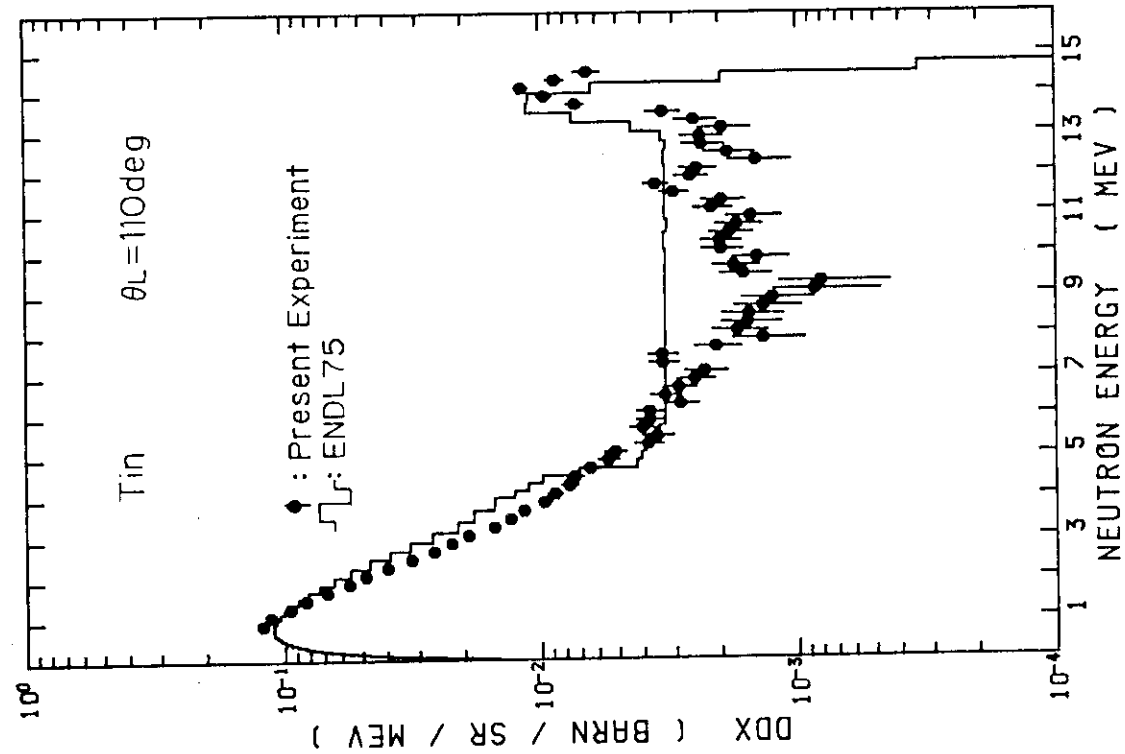


Fig.S-11 Double differential neutron emission cross sections at 110 deg, for Sn

Fig.S-12 Double differential neutron emission cross sections at 120 deg, for Sn

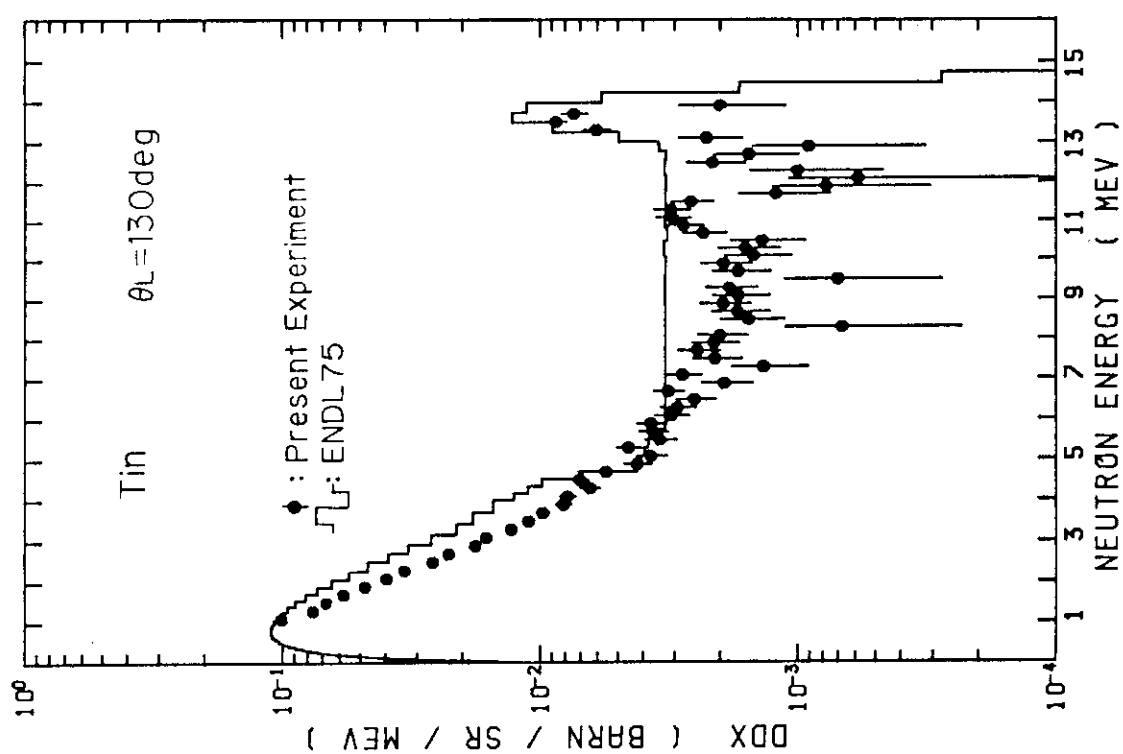


Fig.S-13 Double differential neutron emission cross sections at 130 deg, for Sn

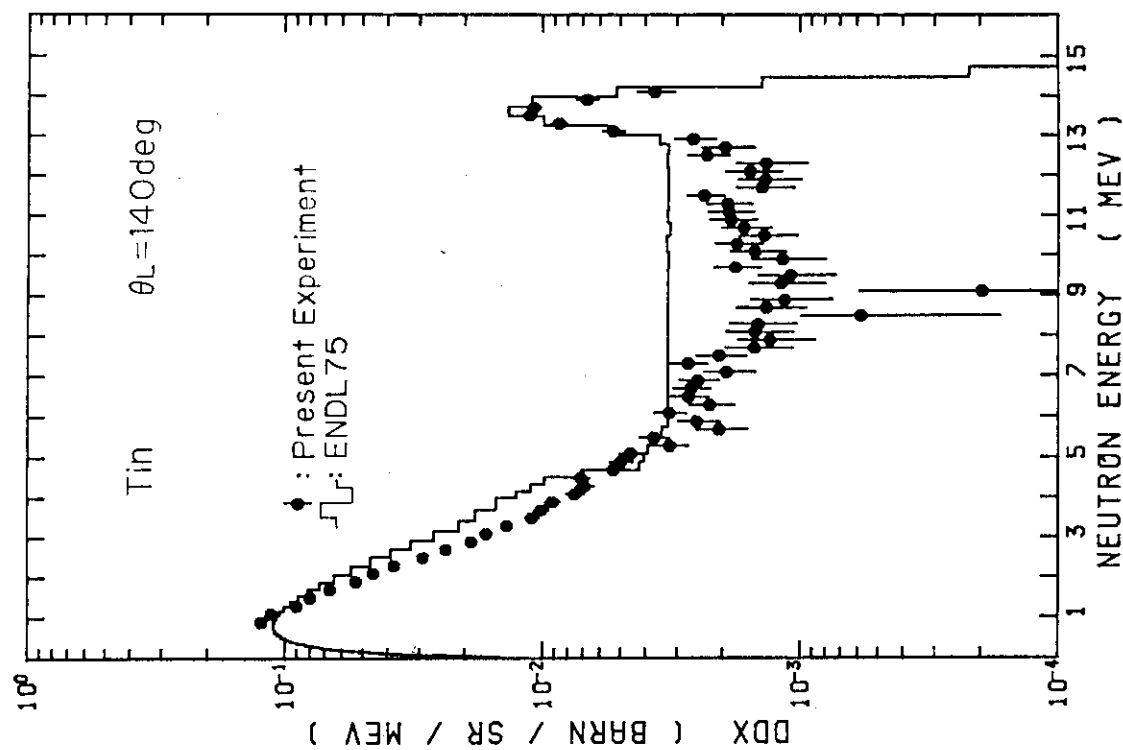


Fig.S-14 Double differential neutron emission cross sections at 140 deg, for Sn

Fig. S-14 Double differential neutron emission cross sections at 140 deg, for Sn

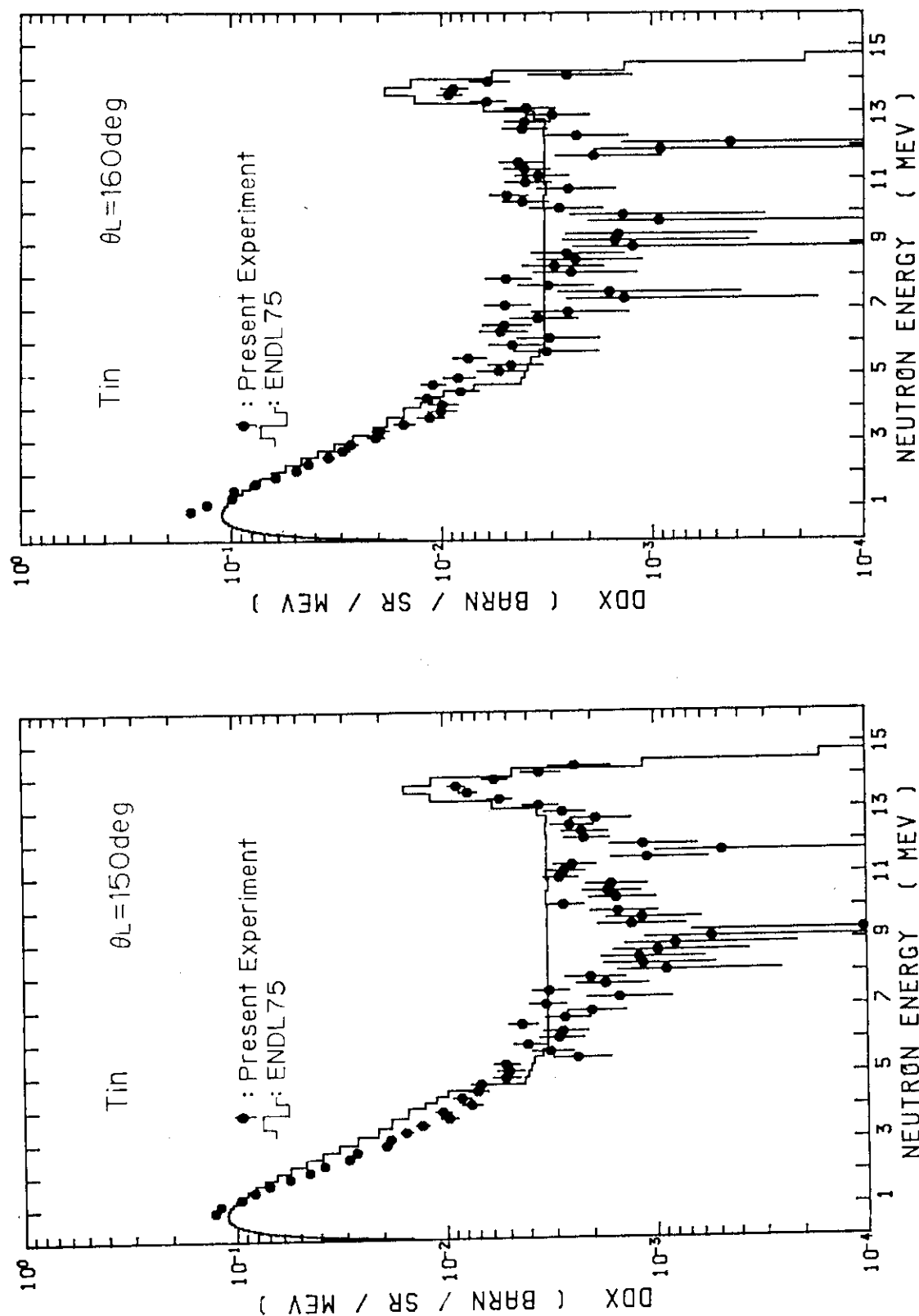


Fig.S-15 Double differential neutron emission cross sections at 150 deg, for Sn

Fig.S-16 Double differential neutron emission cross sections at 160 deg, for Sn

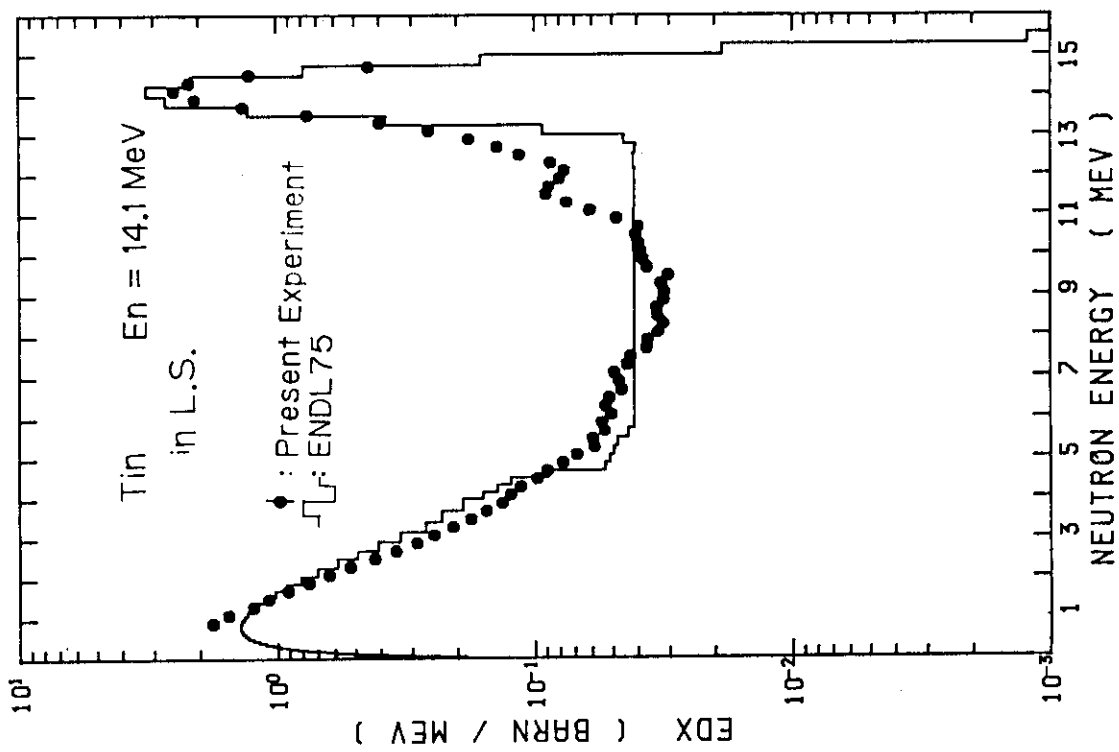


Fig.S-17 Angle-integrated neutron emission spectra in LAB system, for Sn

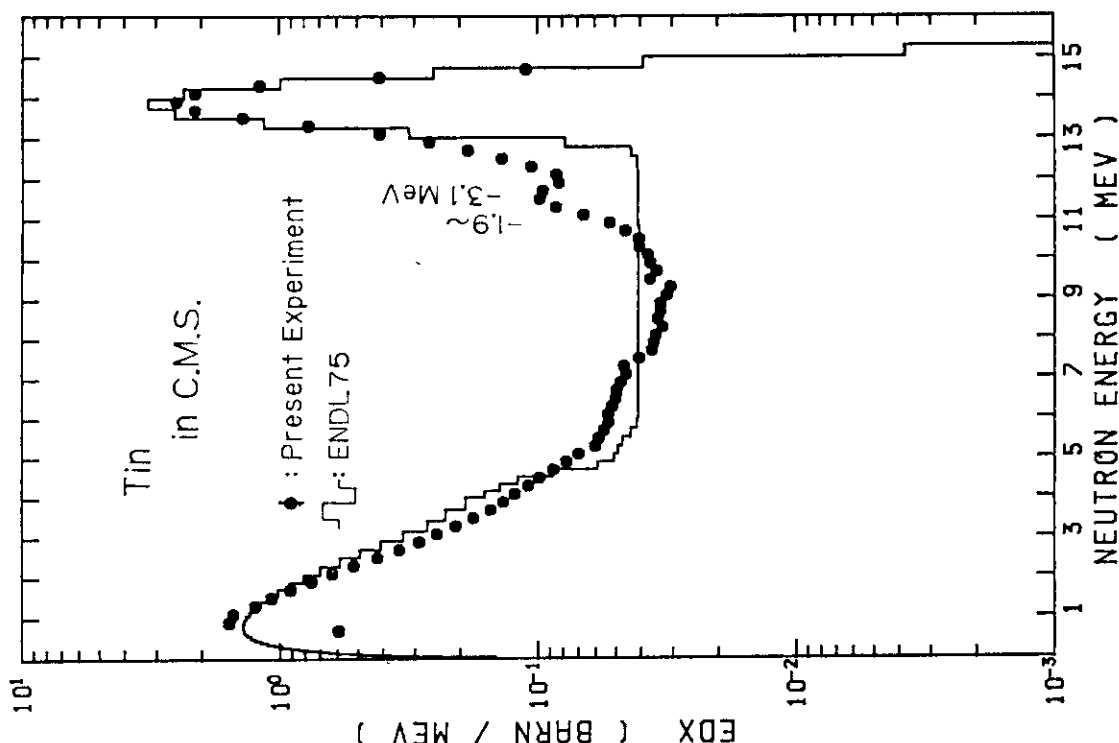


Fig.S-18 Angle-integrated neutron emission spectra in CMS, for Sn

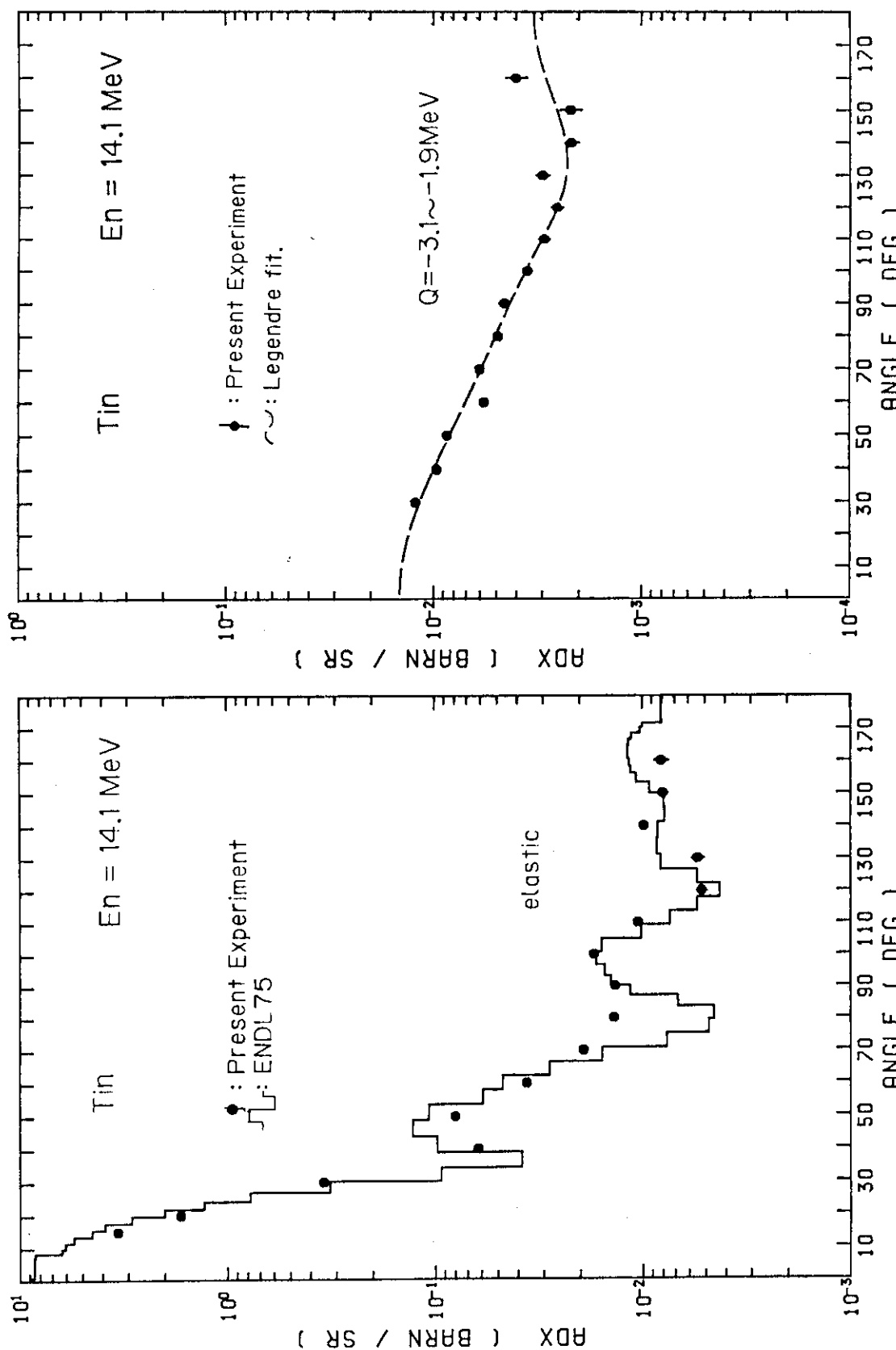


Fig.S-19 Differential elastic scattering cross sections, for Sn

Fig.S-20 Differential inelastic scattering cross sections, for Sn